Depositional architecture of sand-attached and sand-detached channel-lobe transition zones on an exhumed stepped slope mapped over a 2500 km^2 area

Willem C. Van der Merwe[1,*], David M. Hodgson,[2,†], Rufus L. Brunt[3], and Stephen S. Flint[3]
[1]*Stratigraphy Group, Department of Earth, Ocean and Ecological Sciences, University of Liverpool, Liverpool L69 3GP, UK*
[2]*Stratigraphy Group, School of Earth and Environment, University of Leeds, Leeds LS2 9JT, UK*
[3]*Stratigraphy Group, School of Earth, Atmospheric and Environmental Sciences, University of Manchester, Manchester M13 9PL, UK*

ABSTRACT

The geomorphology and seismic stratigraphy of deep-water clastic systems from slope valleys through channel-levee systems to basin-floor fans have been observed and described in modern and ancient subsurface examples around the world. However, the distribution of sedimentary facies, grain size, and small-scale architectural elements remains poorly constrained. Extensive exposures (>2500 km^2) of four stacked deep-water composite sequences have been mapped from heterolithic channel-levee systems on the slope to sand-rich basin-floor deposits. The data set from Units C–F of the Fort Brown Formation in the Permian Laingsburg depocenter of South Africa permits a unique opportunity to document and compare their depositional architecture at a high resolution for tens of kilometers downdip.

Isopach thickness maps indicate that compensational stacking across multiple stratigraphic scales occurs on the basin floor, whereas preferred axial pathways were present on the slope, leading to subvertical stacking patterns. Units C and D are sand-attached systems; slope valley systems are mapped to pass transitionally downslope through levee-confined channels to lobe complexes over distances of >30 km. The slope valley fills of Units E and F, however, are separated from their downdip sand-rich lobe complexes by a thin, sand-poor tract several kilometers in length and are termed sand detached. Locally, this sand-poor tract is characterized by a distinctive facies association of thin-bedded turbidites with numerous scours mantled with rip-up clasts, and a top surface that includes megaflutes and remobilized sediments. This assemblage is interpreted to indicate a widespread area of sand bypass.

This unique data set provides an exploration-scale insight and understanding of how different segments of a prograding slope evolved over time in terms of gradient, physiography, and hence the degree to which sand was stored or bypassed to the basin floor, and the evolution from sand-attached to sand-detached systems. The development of sand-detached systems suggests that a steeper gradient formed, possibly related to developing underlying structure, that led to the development of a stepped slope profile. The study highlights that updip stratigraphic trapping at reservoir scale can occur with minor bathymetric changes.

INTRODUCTION

The seminal first-generation depositional models for deep-water systems were developed from low-resolution seismic and seabed data sets and fragmented outcrop belts (e.g., Normark, 1970, 1978; Mutti and Ricci Lucchi, 1972; 1975; Walker, 1978; Mutti and Normark, 1987, 1991). The advent of three-dimensional (3D) reflection seismic data sets (e.g., Posamentier and Kolla, 2003; Saller et al., 2004; Deptuck et al., 2007; Catterall et al., 2010; Armitage et al., 2012; Saller and Dharmasamadhi, 2012) and high-resolution seabed imagery (e.g., Twichell et al., 1992; Savoye et al., 2000; Fildani and Normark, 2004; Jegou et al., 2008; Maier et al., 2011; MacDonald et al., 2011) has revolutionized our appreciation of the inherent variability and complexity in the physiography and anatomy of submarine systems dominated by sediment gravity flows. The roles of dynamic seabed substrates (e.g., Prather et al., 1998; Mayall et al., 2006; Clark and Cartwright, 2009), depositional relief (e.g., Posamentier and Walker, 2006), inherited bathymetric perturbations (e.g., Adeogba et al., 2005; Olafiranye et al., 2013), differential compaction (e.g., Koša, 2007), compensational stacking (e.g., Prélat et al., 2009), and channel avulsion (Armitage et al., 2012) have been shown to be primary controls on the physiology and seismic stratigraphy of submarine slope and basin-floor systems.

Conceptually, basin-floor fans have been classified as either (channel) attached (Type I of Mutti, 1985; Fugelli and Olsen, 2005a, 2005b) or coupled (Gardner et al., 2003), or as (channel) detached (Type II of Mutti, 1985; Fugelli and Olsen, 2005a, 2005b) or decoupled (Gardner and Borer, 2000). This distinction is based on the nature of the channel-lobe transition zone (CLTZ), which has been widely identified from modern systems (e.g., Mutti and Normark, 1987, 1991; Wynn et al., 2002; MacDonald et al., 2011). In an attached system, there is a physical continuity and lithological connectivity between the channels and lobes, whereas in a detached system there is a widespread area dominated by erosional processes and sediment bypass between the channels and lobes. Detached lobes have been identified associated with early-stage avulsion in modern systems offshore California (Fildani and Normark 2004). Sand-detached systems can be inferred using amplitude responses in 3D seismic data (e.g., Jackson et al., 2008), but their recognition and description at outcrop have not been achieved.

Despite technological advances in subsurface imaging, the detailed analysis of exhumed deep-water systems at outcrop is still essential (Mutti and Normark, 1987) to provide information on sedimentary processes (e.g., Chapin et al., 1994; Pickering and Corregidor, 2005; Jobe et al., 2012), the stacking patterns and geometry

*Present address: Nexen Petroleum UK Limited, Prospect House, 97 Oxford Road, Uxbridge, UB8 1JG, UK
†Corresponding author: d.hodgson@leeds.ac.uk

Geosphere; December 2014; v. 10; no. 6; doi:10.1130/GES01035.1; 14 figures.
Received 3 February 2014 ♦ Revision received 19 August 2014 ♦ Accepted 26 September 2014

of subseismic elements (e.g., Beauboeuf et al., 2000; Abreu et al., 2003; Schwarz and Arnott, 2007; Kane et al., 2007; Prélat et al., 2009), and the intrinsic controls on the anatomy of deep-water systems (e.g., Mutti 1985; Hodgson and Haughton, 2004; Moody et al., 2012; Burgreen and Graham, 2014). However, outcrops used as analogs are commonly isolated two-dimensional exposures, or have limited across-strike or downdip correlation potential, meaning that their paleogeographic context within the regional depositional architecture of a deep-water system is uncertain. The long-distance analysis of facies distributions and thicknesses to constrain the depositional architecture of deep-water systems at outcrop is rare but has been achieved for individual beds (e.g., Hesse, 1974; Remacha and Fernández, 2003; Amy and Talling, 2006; Sumner et al., 2012). Notable exceptions where deep-water systems have been mapped and correlated for tens of kilometers downslope are illustrated in Figure 1 and include the Brushy Canyon Formation of Texas (e.g., Beauboeuf et al., 2000; Gardner et al., 2003), the Magallanes Basin, Chile (e.g., Hubbard et al., 2010; Bernhardt et al., 2011), and the Karoo Basin, South Africa (e.g., Johnson et al., 2001; Grecula et al., 2003; Sixsmith et al., 2004; Figueiredo et al., 2010; Brunt et al., 2013a).

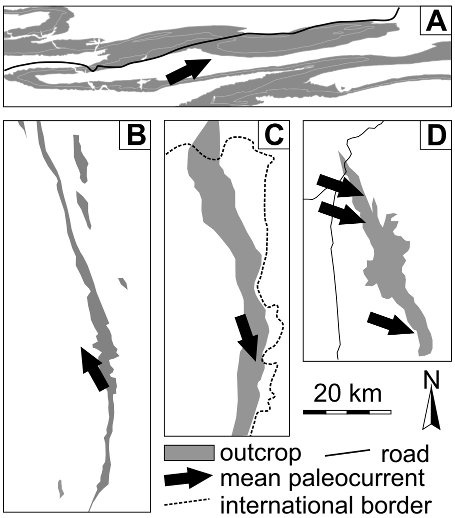

Figure 1. Simplified outcrop patterns of large-scale (>2500 km²) exhumed deep-water systems that have been mapped and correlated from updip to downdip. All maps are at the same scale. (A) The Laingsburg depocenter (Karoo Basin, South Africa), including the Laingsburg and Fort Brown Formations. (B) The Pab Sandstone (Pakistan; adapted from Eschard et al., 2003). (C) The Tres Pasos Formation (Chile; adapted from Shultz et al., 2008). (D) The Brushy Canyon Formation (Texas, USA; adapted from Gardner et al., 2003). Note the orientation of the outcrop belt relative to mean paleocurrent direction. The postdepositional folding in the Karoo Basin provides good strike and dip outcrop control.

In the Karoo Basin, the extensive exposures of middle and/or upper slope to basin-floor deposits in the Laingsburg depocenter have permitted the mapping and correlation of four stacked deep-water composite sequences over a >2500 km² area. A major advantage of the Karoo Basin outcrop belt is that the post-depositional folding and orientation of paleoflow allow stacked stratigraphic units to be mapped across strike and downdip from the submarine slope channel-levee system to their genetically related basin-floor deposits (Fig. 1). The unique compiled data set permits for the first time (1) documentation of the detailed depositional architecture of successive large-scale deep-water systems from slope channel-levee systems to distal basin-floor fans, (2) assessment of the role of depositional relief on sediment dispersal patterns at a range of scales, (3) identification and documentation of an exhumed stepped slope profile, and (4) differentiation between sand- or sandstone-attached and detached channel-lobe transition zones, and consideration of the subsurface implications for these system types.

STRATIGRAPHIC SETTING

The Karoo Basin is interpreted as a thermal sag basin (Permian) that evolved into a retro-arc foreland basin during the Triassic (Tankard et al., 2009). In the Laingsburg depocenter the 1.3-km-thick Permian Ecca Group comprises a basal mudrock succession (Vischkuil Formation; Van der Merwe et al., 2009) (Fig. 2), overlain by a sand-prone basin-floor to slope succession (Laingsburg and Fort Brown Formations, respectively; Grecula et al., 2003; Sixsmith et al., 2004; Flint et al., 2011; Brunt et al., 2013b). Mapping and correlating the deep-water stratigraphy in the Laingsburg area is aided by the regional exposure and extent of mudstone units (15–50 m thick) that thin

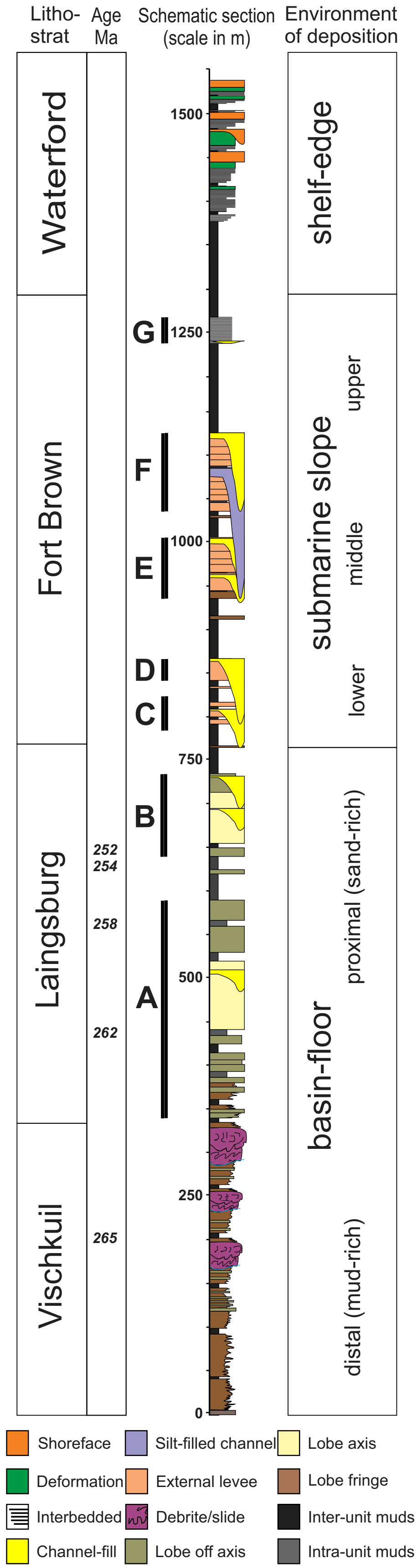

Figure 2. Schematic stratigraphic (lithostrat is lithostratigraphy) section of the Ecca Group in the Laingsburg area (Karoo Basin, South Africa). The overall shallowing-upward trend records the long-term progradation of the Karoo Basin margin to the northeast. Units C–F in the Fort Brown Formation are the focus of this study. Ages are from Fildani et al. (2009).

gradually and evenly basinward (~1 m/km). The regional extent of the mapped mudstones, and their gradual basinward taper, leads to an interpretation that they contain the deep-water equivalent of maximum flooding surfaces (Van der Merwe et al., 2010; Flint et al., 2011). The mudstones separate sandstone-prone units (Units A–F) that can vary abruptly in thickness and sedimentary facies both laterally and down-dip (Fig. 2). Units A–F have been interpreted to represent four composite sequence sets, each composed of three composite sequences (Flint et al., 2011). This paper focuses on the upper two composite sequence sets, Units C–D and Units E–F (Fig. 2). Each sand-prone unit represents a lowstand sequence set, the overlying hemipelagic mudstone package forming the combined transgressive and highstand sequence set. As demonstrated for Unit C (Di Celma et al., 2011; Hodgson et al., 2011), Unit D (Brunt et al., 2013a), and Units E and F (Figueiredo et al., 2010), each lowstand sequence set is composed of three depositional sequences, each including a sandstone-dominated lowstand systems tract (referred to as a subunit, such as C1, C2, C3) and a genetically related and regionally extensive 1–5-m-thick muddy transgressive and highstand systems tract. Depositional dip control for Units C–F extends from middle and/or upper slope to distal basin-floor fan, a distance of 80–100 km (Fig. 3).

ARCHITECTURAL ELEMENTS AND SEDIMENTARY FACIES

Numerous previous studies have described and interpreted the sedimentary facies and architectural elements of the basin floor (Sixsmith et al., 2004; Van der Merwe et al., 2009, 2010, 2011; Prélat and Hodgson, 2013), submarine channel-levee systems (Grecula et al., 2003; Figueiredo et al., 2010, 2013; Hodgson et al., 2011; Brunt et al., 2013a), and the transitions (Di Celma et al., 2011; Brunt et al., 2013b) in the Laingsburg and Fort Brown Formations. In basin-floor settings, four main environments of deposition are used to characterize the internal sedimentary facies distribution within lobes, based on field work in the neighboring Tanqua depocenter (Prélat et al., 2009; Groenenberg et al., 2010). Lobe axes are represented by amalgamated fine-grained sandstones, lobe off-axis settings are represented by stratified with planar to wavy laminated fine-grained sandstones, and lobe fringes are represented by thin-bedded current ripple–laminated sandstones and siltstones, commonly rich in a range of hybrid bed types (Hodgson, 2009). Distal lobe fringe deposits comprise thinly bedded graded siltstones (Fig. 4). Where channels cut through basin-floor lobes the architecture of their fill tends to be sand rich and simple (e.g., Sixsmith et al., 2004; Brunt et al., 2013b). On the submarine slope, channelized portions are represented by a complicated stratigraphy with closely spaced, crosscutting erosion surfaces. In axial positions the erosion surfaces are overlain by mudstone clast conglomerates, amalgamated fine-grained sandstones, and mass flow deposits (chaotic and folded strata; Fig. 4). Toward the margins of channel fills thin-bedded ripple laminated sandstone beds fine and thin onto erosional surfaces (Pringle et al., 2010; Hodgson et al., 2011; Fig. 4). Internal levees, which are formed by deposits of flows that spill out of channel confinement, but are confined by the margins of the larger valley, comprise climbing ripple cross-laminated sandstones with multiple flow directions and centimeters-thick siltstones (Kane and Hodgson, 2011; Fig. 4). Siltstone-rich external levees form wedges that fine and thin away from parent channel systems, which commonly comprise basal climbing ripple laminated very fine grained and fine-grained sandstones overlain by planar laminated siltstones and mudstones to form fining- and thinning-upward packages (Kane and Hodgson, 2011; Morris et al., 2014a; Fig. 4).

REGIONAL DEPOSITIONAL PATTERNS

Regional sedimentary facies patterns and architectural descriptions were recorded in seven regional scale (60–90 km) depositional

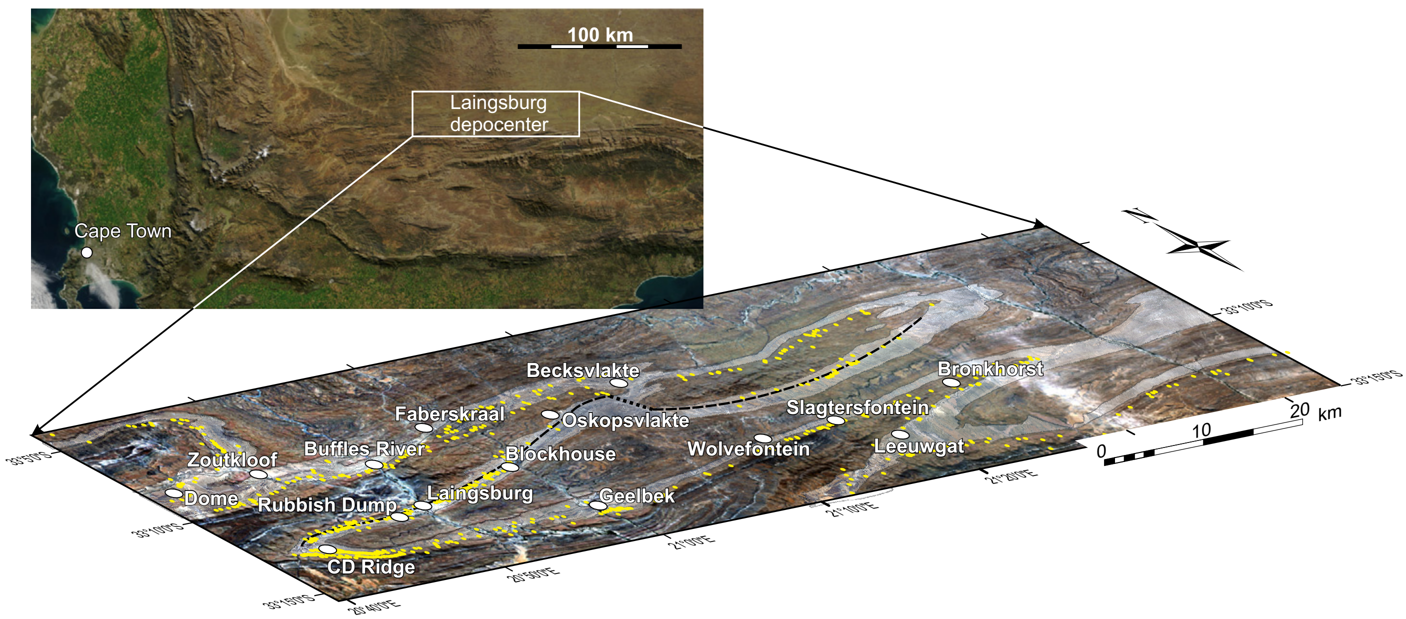

Figure 3. Location of the study area and outcrop pattern (in gray). Overall paleoflow direction is to the northeast and east and exposures along postdepositional fold limbs provide a series of dip sections as much as 100 km long. Basal positions of logged sections are marked in yellow. The line of section of Figure 5 is shown by the black dashed line. Aerial photographs are from NASA Visible Earth (National Aeronautics and Space Administration, http://visibleearth.nasa.gov/; regional scale) and Chief Directorate: National Geo-spatial Information, South Africa (http://www.ngi.gov.za/; Laingsburg depocenter).

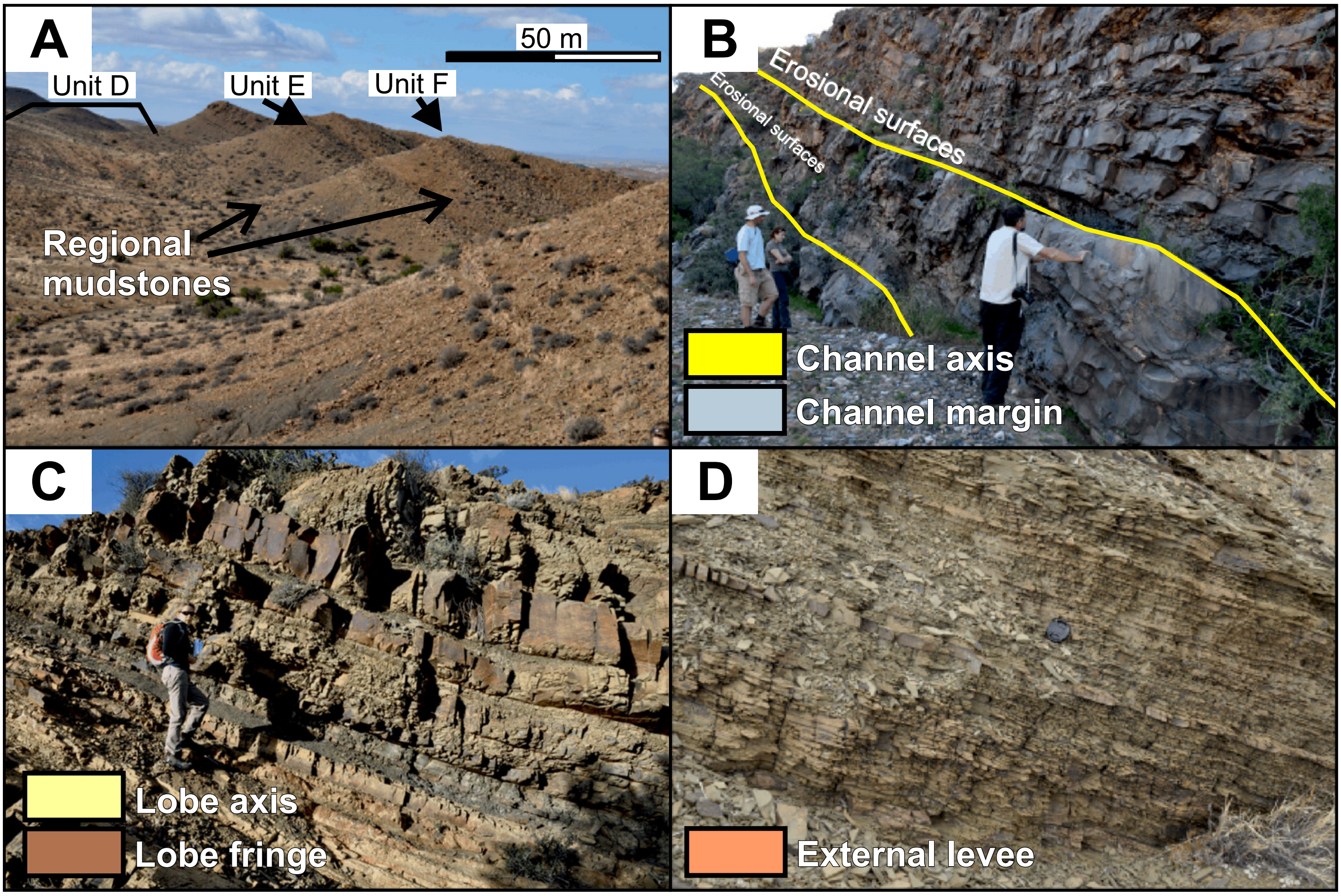

Figure 4. Examples of the main facies associations and their color coding on the correlation panel (Fig. 5) and maps (Figs. 6, 7, 8, and 10). (A) The mapped regional mudstone drapes over the sand-prone units are interpreted as combined transgressive and highstand sequence sets. (B) Channel fills vary from sandstone filled (base of slope) to mixed lithologies in slope settings. Channel-margin deposits are commonly thin bedded. (C) Lobe complexes dominate the downdip areas of lowstand sequence sets and axis, off-axis, and fringe settings are recognized. (D) Thin-bedded silt-rich external levees are volumetrically the most common component on the submarine slope.

dip–parallel correlation panels located on the fold limbs (from south to north, Floriskraal South, Floriskraal North, Baviaans South, N1 Dome South, Baviaans North, Faberskraal South, Faberskraal North). The database includes more than 1000 measured sections (Fig. 3) that were correlated by walking out key surfaces and units (typically the mudstones between each sand-prone unit). The correlation panels follow the west-east–trending limbs of the main postdepositional folds, and careful tracing of markers around the closures of these folds provides high confidence correlation between fold limbs (Figs. 3 and 5).

Mapped thickness distributions (isopachs) were created by fitting a surface to thickness values extracted from the logged sections. The surfacing operation was conducted in ArcGIS using the simple kriging tool within the Geostatistical Wizard (http://resources.arcgis.com/en/home/). Generally, a 15% trend removal was used to force the software to honor the spot thicknesses. Output maps are extended to the north, east, south, and west extremities of the input data by the surfacing algorithm, which creates rectangular maps that may extend beyond the edge of the input data. Unrealistic contour values have been removed from these edge areas. Paleogeographic maps are based on the distribution of sedimentary facies and architectural elements, and illustrate the gross depositional environment for the stratigraphic interval presented (Figs. 4 and 5). One constraint due to the postdepositional folding is that the noses of the folds determine the absolute present-day limits of the stratigraphy. The isopach and paleogeographic maps presented have not been palinspastically restored. The amount of north-directed tectonic shortening across the study areas is estimated as 10%–20%, and decreases to the north. This is consistent with published amounts of shortening (Newton 1992), and indicates that the present-day 2500 km^2 study area was <3000 km^2. The gross depositional environment maps therefore provide a reasonable representation of the systems at the time of deposition, although the rate of north-south thinning in isopach thickness maps is exaggerated.

Unit C: Regional Depositional Pattern

The most proximal preserved part of the lowstand sequence set of the Unit C composite sequence is located at the CD Ridge, Baviaans syncline (Di Celma et al., 2011; Fig. 3); it has been mapped to the north for 20 km and to the east for 90 km. Unit C has a defined southern margin; deposits are thin to absent south of the northern limb of the Baviaans syncline. Mapping shows physical continuity and connectivity

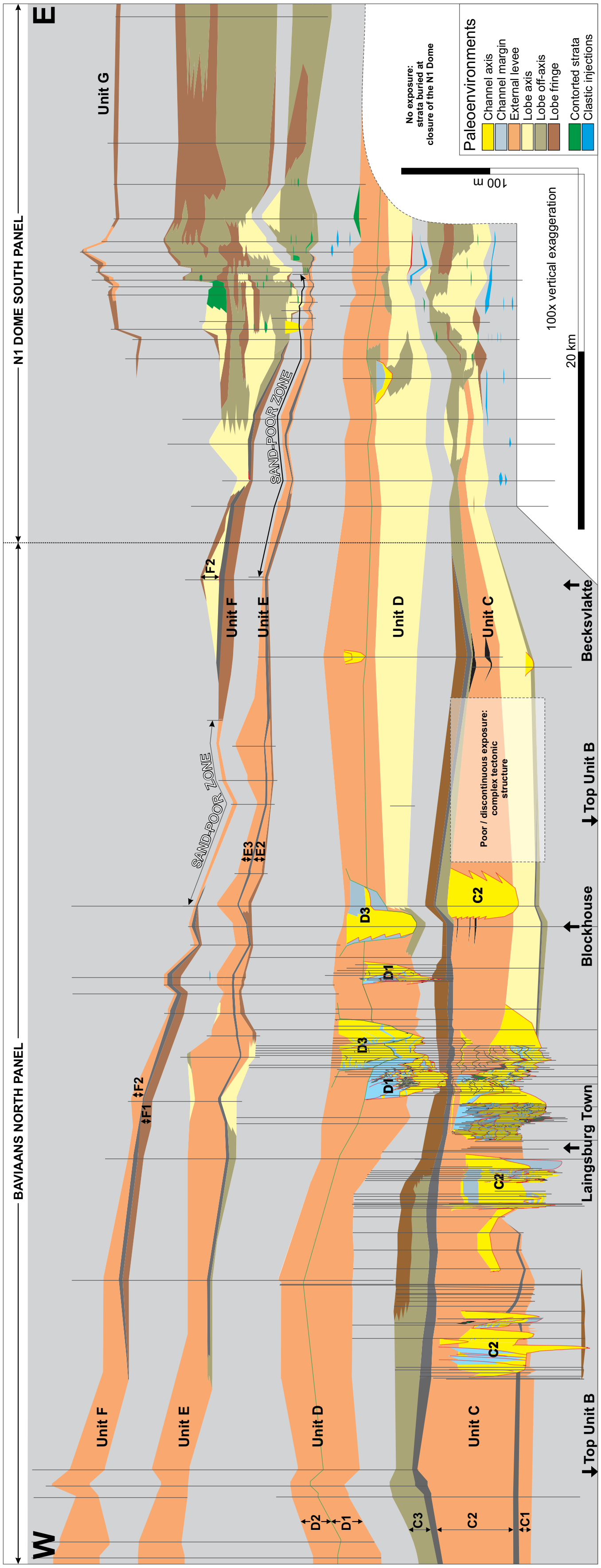

Figure 5. Regional (80 km long) depositional dip section correlation panel showing the geometry and facies associations in Units C, D, E and F, each of which is interpreted as a lowstand sequence set. The corresponding transgressive and highstand sequence sets are combined in the mudstone drape that overlies each unit; together, each unit and overlying drape are interpreted as a composite sequence (Flint et al., 2011). Note the general downdip (basinward) trend from channel-levee complexes (orange) to distributive lobe complexes (pale yellow). Vertical black lines mark the position of logged sections.

of sand-rich strata between updip channel-levee systems and downdip lobes for each lowstand systems tract (Fig. 5).

C1 Lowstand Systems Tract: Updip Section

On the northern limb of the Baviaans syncline C1 is a thin (as much as 5 m thick) package of thinly bedded heterolithic deposits, which progressively thin eastward toward the Laingsburg rubbish dump (Di Celma et al., 2011).

C1 Lowstand Systems Tract: Downdip Section

Downdip (northeast) C1 dramatically thickens and coarsens toward Zoutkloof, where a maximum recorded thickness (64 m) is interpreted as the centroid to a lobe complex (Fig. 6A). C1 thins and fines to the west, east, and north, away from Zoutkloof (Di Celma et al., 2011) and downlaps out east of the Laingsburg town area (Fig. 6A).

C2 Lowstand Systems Tract: Updip Section

Subunit C2 is dominated by a >2-km-wide erosive based and levee-bounded slope channel complex set (Hodgson et al., 2011). The overall stacking pattern of channel fills and channel complex fills within the set is early lateral and late aggradational (Hodgson et al., 2011). The distribution of paleocurrents shows a trend between east and north-northeast for individual channels within the complex set. Immediately downdip of the CD Ridge, the Unit C2 axis divides into a series of smaller channel complexes separated laterally by external levee deposits along the northern limb of the Baviaans syncline (Fig. 6B). Mapping of C2 to the north indicates that the channel complexes turn eastward (Di Celma et al., 2011), possibly due to bathymetric relief on the underlying C1 lobe complex located to the north at Zoutkloof locality (Fig. 6B).

C2 Lowstand Systems Tract: Downdip Section

A transition to lobe deposits occurs ~20 km downdip of the CD Ridge, where amalgamated sandstones at the base of C2 are interpreted as frontal lobe deposits. External levee deposits overlie stacked lobes for a further 20 km downdip, forming the thickest C2 accumulations (~60 m) (Fig. 6B). At Geelbek and Wolwefontein, C2 consists of tabular bedded sandstones commonly associated with linked debrites, which are interpreted to have been deposited in a lobe fringe environment. C2 is absent in the Floriskraal syncline farther to the southeast (Fig. 6B).

C3 Lowstand Systems Tract: Updip Section

Subunit C3 has the smallest geographic extent. At the CD Ridge, C3 crops out as thin interbedded very fine grained sandstones and siltstones ~14 m thick, interpreted as a frontal lobe complex (Morris et al., 2014b). The frontal

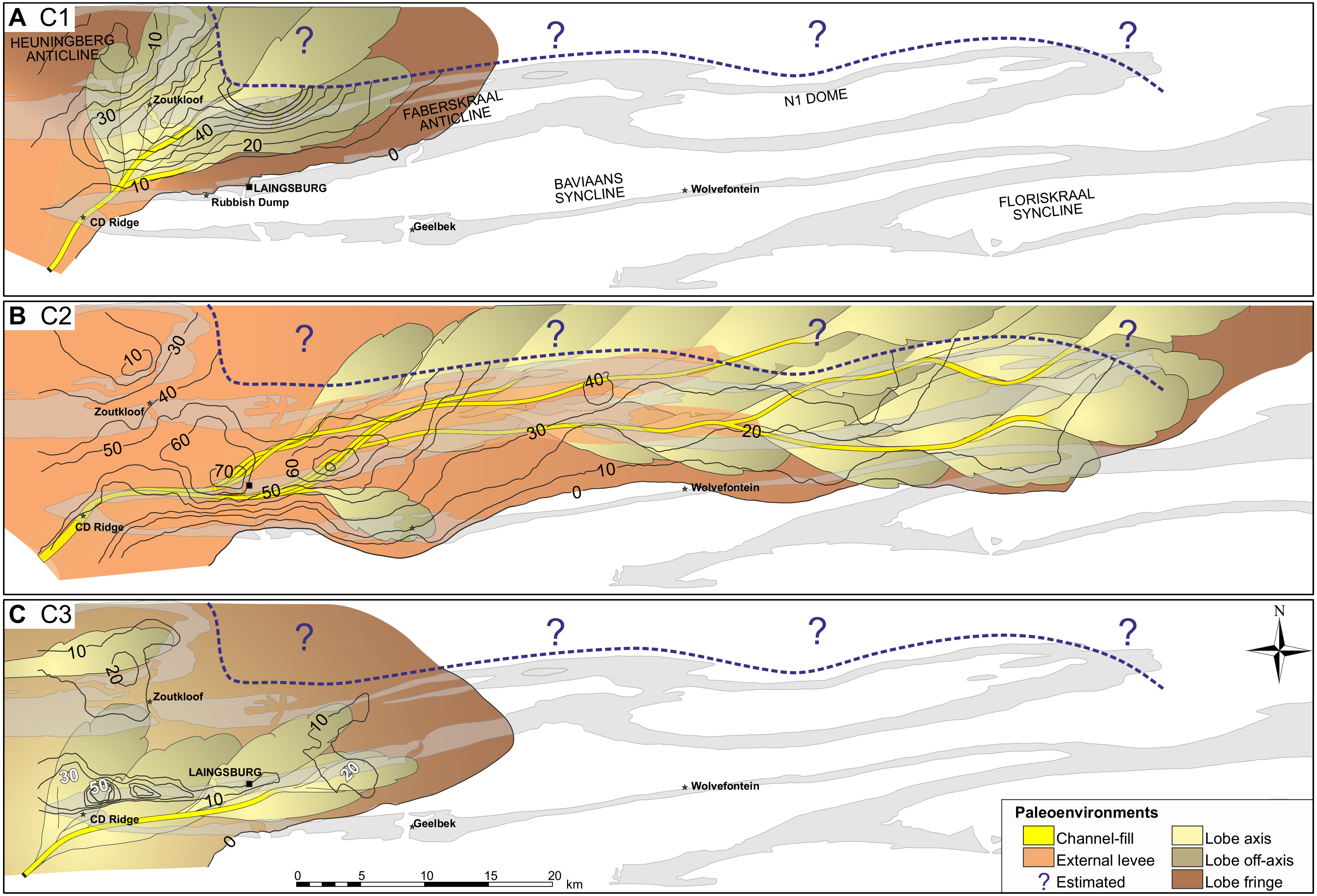

Figure 6. Thickness isopach and gross depositional environment maps for the individual constituent lowstand systems tracts (C1, C2, and C3) of the Unit C lowstand sequence set. Positions of channels are tied to outcrop location, but lobe boundaries are not precise positions. The grayed areas show the outcrop control along the limbs of postdepositional folds over a study area of 2500 km². Note the clear progradational to retrogradational stacking pattern with maximum sand delivery to the basin floor during the C2 lowstand systems tract.

lobe complex thickens considerably directly north of the CD Ridge, at the north side of the Baviaans syncline, and thins abruptly to the east and west (Morris et al., 2014b; Fig. 6C). Bathymetric confinement, possibly by the C1 lobe complex to the north in the Zoutkloof area (Di Celma et al., 2011) and earlier channel fills and associated levees to the C2 axis, are thought to have influenced the local thickness.

C3 Lowstand Systems Tract: Downdip Section

C3 continues for 28 km downdip of the CD Ridge, with a general thinning and fining-eastward pattern, becoming thicker and sandier locally (Fig. 6C); it displays characteristics of a terminal lobe complex (Morris et al., 2014b). A second, east-trending system in C3 is present across strike to the north (Fig. 6C), supplying clastic material to the Heuningberg anticline area (Di Celma et al., 2011).

Unit D: Regional Depositional Pattern

The lowstand sequence set of the Unit D composite sequence is represented in the western, updip area by a 120-m-thick slope valley fill that cuts into earlier Unit D external levee deposits and completely truncates the C–D mudstone and Unit C along the CD Ridge (Hodgson et al., 2011). The valley fill is bounded by wedge-shaped external levees that extend as much as 10 km laterally away from the valley. The D valley extends east-northeast down the Baviaans syncline, emerging on the north limb just east of Laingsburg. At this point the system is a levee-confined channel complex set, but with sufficient basal incision to truncate the C–D mudstone and subunit C3 (Brunt et al., 2013a). This downdip trend of decreasing incision has been interpreted as a response to reducing gradient downslope. Regional mapping has extended the knowledge of Unit D for an additional 90 km to the east (obliquely downdip), and the depositional architecture is apparent (Fig. 5). Although there are no regional internal mudstones within the lowstand sequence set, abrupt vertical changes in facies association and architectural elements, and therefore relative geographic position in the system, are used to subdivide Unit D into three sequences. The absence of regional internal mudstones limits confidence in identification of relative ages within the D composite sequence. Mapping shows continuity of sand-rich strata between updip sand-prone channel fills and downdip sand-prone lobes at composite sequence scale.

D1 Lowstand Systems Tract: Updip Section

In the western study area, D1 is marked by external levee deposits as much as 8 m thick and remnants of early frontal lobes (Hodgson et al., 2011). The interpreted genetically related channel system to the D1 levees has been removed by the later slope valley development in the CD Ridge area (Hodgson et al., 2011).

D1 Lowstand Systems Tract: Downdip Section

D1 is represented by lobe deposits in the downdip half of its outcrop belt. The main development of lobe deposits is east of the Blockhouse (Fig. 7A; Brunt et al., 2013a). These successions show a range of facies associations, stratigraphic organization indicative of alternating lobe axis and/or off axis and lobe fringe, and thicknesses (1–8 m) similar to lobes described by Prélat and Hodgson (2013) in the underlying Unit A.

D2 Lowstand Systems Tract: Updip Section

In the updip CD Ridge area D2 is interpreted as the development of the main slope valley erosional surface and the early, low accommodation-fill component (Hodgson et al., 2011). Regional correlation and mapping show that D2 deposits are confined to updip bypass surfaces, passing downdip into very extensive levee systems (Fig. 7B). There are major channel complexes associated with the levees, particularly in the Faberskraal and Slagtersfontein areas (Fig. 7B).

D2 Lowstand Systems Tract: Downdip Section

Significant thicknesses of exposed lobe deposits are in the far downdip Floriskraal syncline and N1 Dome East area (Fig. 7B), which are partially correlated to the major channel complexes in the Faberskraal and Slagtersfontein areas. The absence of internal mudstones there indicates uncertainty in the identification of the contact between D1 and D2 deposits in the lobe-dominated successions, such that the map-view reconstructions are a preferred interpretation.

D3 Lowstand Systems Tract: Updip Section

D3 deposits are interpreted to represent the upper, more aggradational part of the fill of the slope valley and the upper part of the external levee complex in the CD Ridge (Hodgson et al., 2011), although the valley remained underfilled after this time (Fig. 7C).

D3 Lowstand Systems Tract: Downdip Section

Approximately 30 km downdip, D3 is interpreted as the 70-m-thick incised late-stage channel complex at Geelbek (Brunt et al., 2013a). Similar D3 sandy channel complexes are present on the N1 east section and in the Oskopsvlakte area (Fig. 7C). D3 is marked by a channel and levee complex around Leeuwgat and Bronkhorst South.

Unit E: Regional Depositional Pattern

Unit E has been interpreted as a lowstand sequence set and is overlain by the E–F mudstone that represents the linked transgressive and highstand sequence set of the Unit E composite sequence (Figueiredo et al., 2010; Flint et al., 2011; Fig. 2). In the western, updip area, the maximum thickness of Unit E is 100 m, and it comprises three sequences, the lowstand systems tracts of which are named E1, E2, and E3 (Figueiredo et al., 2010; Figs. 8A–8C). Mapping shows that there is no definitive sand connection, although there is physical stratigraphy continuity, between the updip and downdip areas.

E1 Lowstand Systems Tract: Updip Section

The sandstone-dominated deposits of E1 form a frontal lobe cut by E1 aged high-aspect-ratio channels (Figueiredo et al., 2010). As the channels cut 3 m deeper than the regional base of E1 they are thought to be bypass channels, with E1 being a perched (or intraslope) lobe (e.g., Fonnesu, 2003; Adeogba et al., 2005; Bohn et al., 2012).

E1 Lowstand Systems Tract: Downdip Section

Unit E1 is found only in the northwestern part of the study area and does not extend east of Laingsburg (Fig. 8A).

E2 Lowstand Systems Tract: Updip Section

Two subparallel east-west–trending 7–8-m-thick channel fills are flanked by extensive levee wedges (Figueiredo et al., 2010; Fig. 8B). The deeper incision of E2 channels compared to E1 suggests a more proximal channel-levee environment, and therefore a progradational stacking pattern.

E2 Lowstand Systems Tract: Downdip Section

Tabular lobe deposits at the base of Unit E are present to the south of Laingsburg town and continue to thicken toward the east. These lobes are interpreted to have been supplied by an eastward-trending channel in an area now uplifted.

E3 Lowstand Systems Tract: Updip Section

Thick-bedded sandstones overlying erosional surfaces in the northern and central areas are interpreted as eastward-trending slope channel fills. Adjacent medium- and/or thin-bedded heterolithic deposits, which are the predominant facies association in E3, are interpreted as external levee deposits (Figueiredo et al., 2010; Fig. 8C). The thickness and the depth of incision in E3 channels in the southern Heuningberg area suggest more proximal and energetic conditions than in E2 (Fig. 8B).

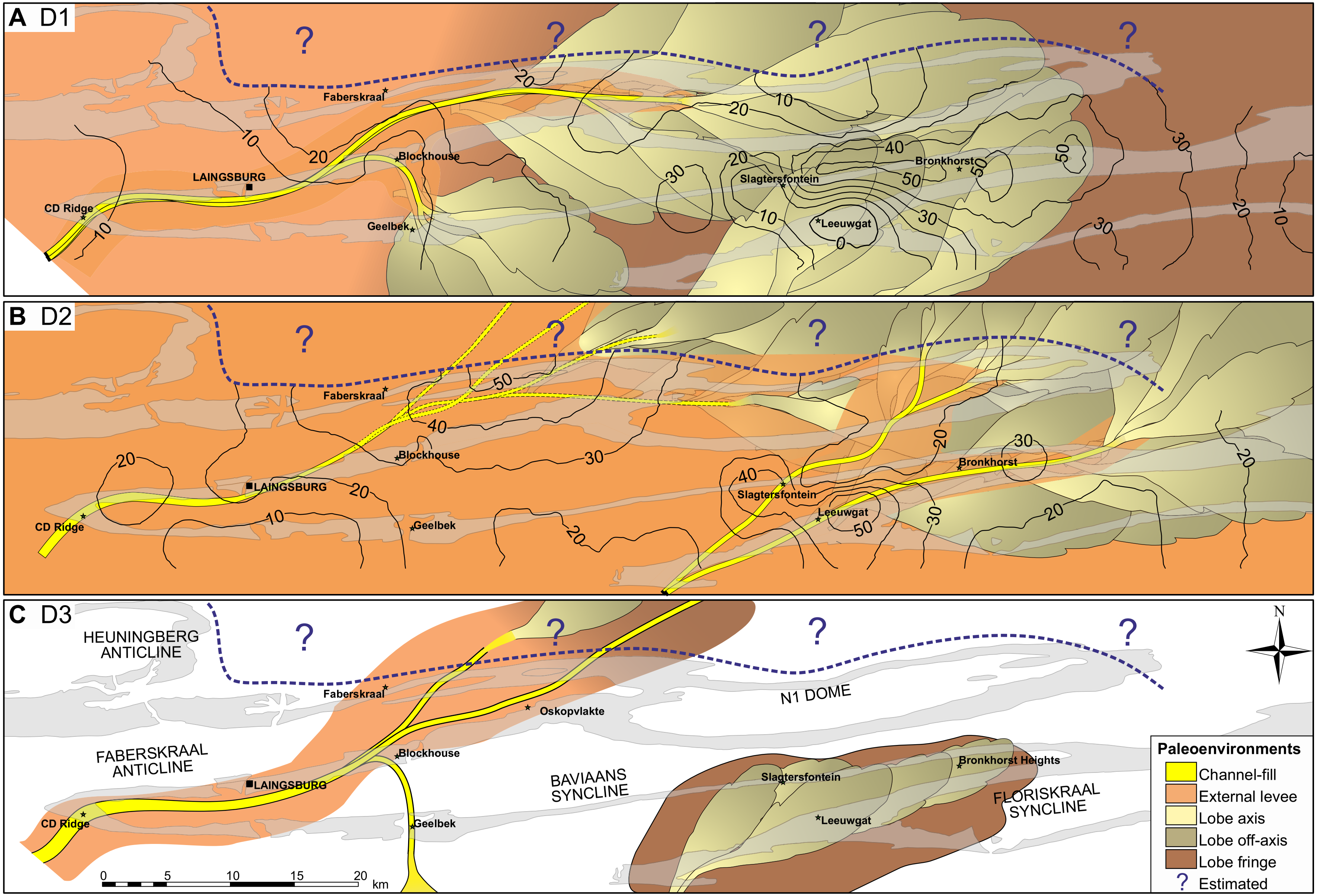

Figure 7. Thickness isopach and gross depositional environment maps for the individual constituent lowstand systems tracts (D1, D2, D3) of the Unit D lowstand sequence set. Positions of channels are tied to outcrop location, but lobe boundaries are not precise positions. A common indicator of progradation is the juxtaposition of external levee over lobe deposits. No isopach contours have been added to D3 due to uncertainties in the division of D2 and D3 in many areas.

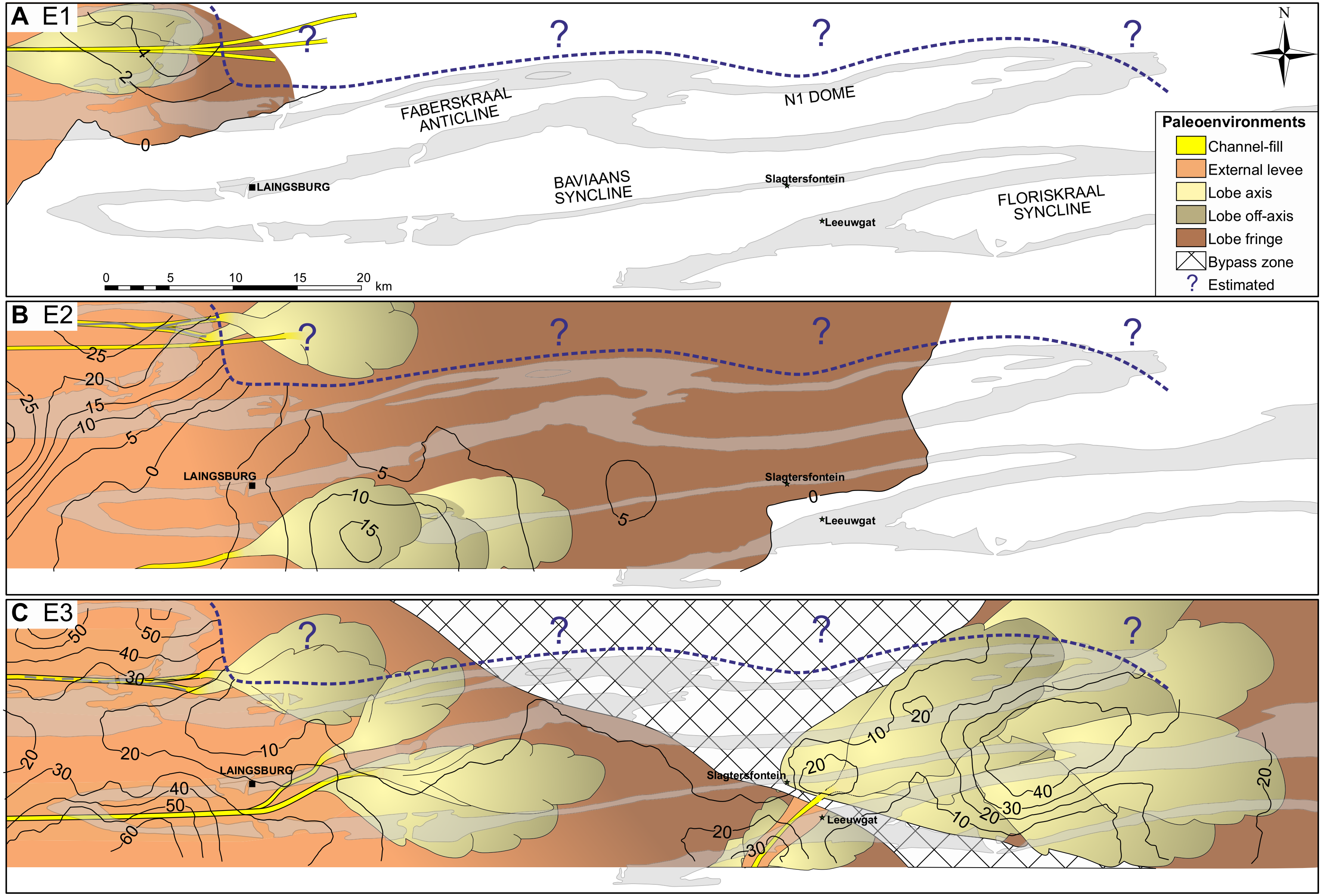

Figure 8. Thickness isopach and gross depositional environment maps for the individual constituent lowstand systems tracts (E1, E2, and E3) of the Unit E lowstand sequence set. Positions of channels are tied to outcrop location, but lobe boundaries are not precise positions. Note the clear progradational trend of successive lowstand systems tracts and the sand- and/or sandstone-detached lobes within E3. Updip data partly from Figueiredo et al. (2010).

E3 Lowstand Systems Tract: Downdip Section

Regional mapping and correlation for E3 show an area of thinning that extends south (across strike) from the N1 Dome through Slagtersfontein to Leeuwgat (Figs. 8B and 9A), with localized scouring and minor deformational features at Slagtersfontein (Figs. 9B, 9C). Lobe deposits are found just updip of the north-south–trending tract of thinning at Leeuwgat (Fig. 8C). Farther east and southeast there is an increase in tabular lobe deposits, interpreted to have been sourced by the slope valley in the northwest (Fig. 8C).

Unit F: Regional Depositional Pattern

Unit F is divided into three sand-prone subunits (F1, F2, and F3 lowstand systems tracts; Figs. 10A–10C) that are separated by two fine-grained units comprising claystone and siltstone interpreted as combined transgressive and highstand systems tracts. (Figueiredo et al., 2010, 2013). Unit F is interpreted as a lowstand sequence set of a composite sequence (Flint et al., 2011). The updip northern area comprises highly erosional slope valley fills >100 m thick, bounded by wedge-shaped external levees that extend for more than 20 km laterally away from the valleys (Figueiredo et al., 2010, 2013). Although there is physical continuity at this stratigraphic level, regional mapping does not indicate a definitive sand connection between updip channelized and downdip lobe-dominated tracts.

F1 Lowstand Systems Tract: Updip Section

The sedimentary facies associations, architecture of the sandstone/siltstone bodies, absence of erosional features and paleocurrent directions in F1 are consistent with the distal fringe of an upper slope distributive system (Figueiredo et al., 2010; Fig. 10A).

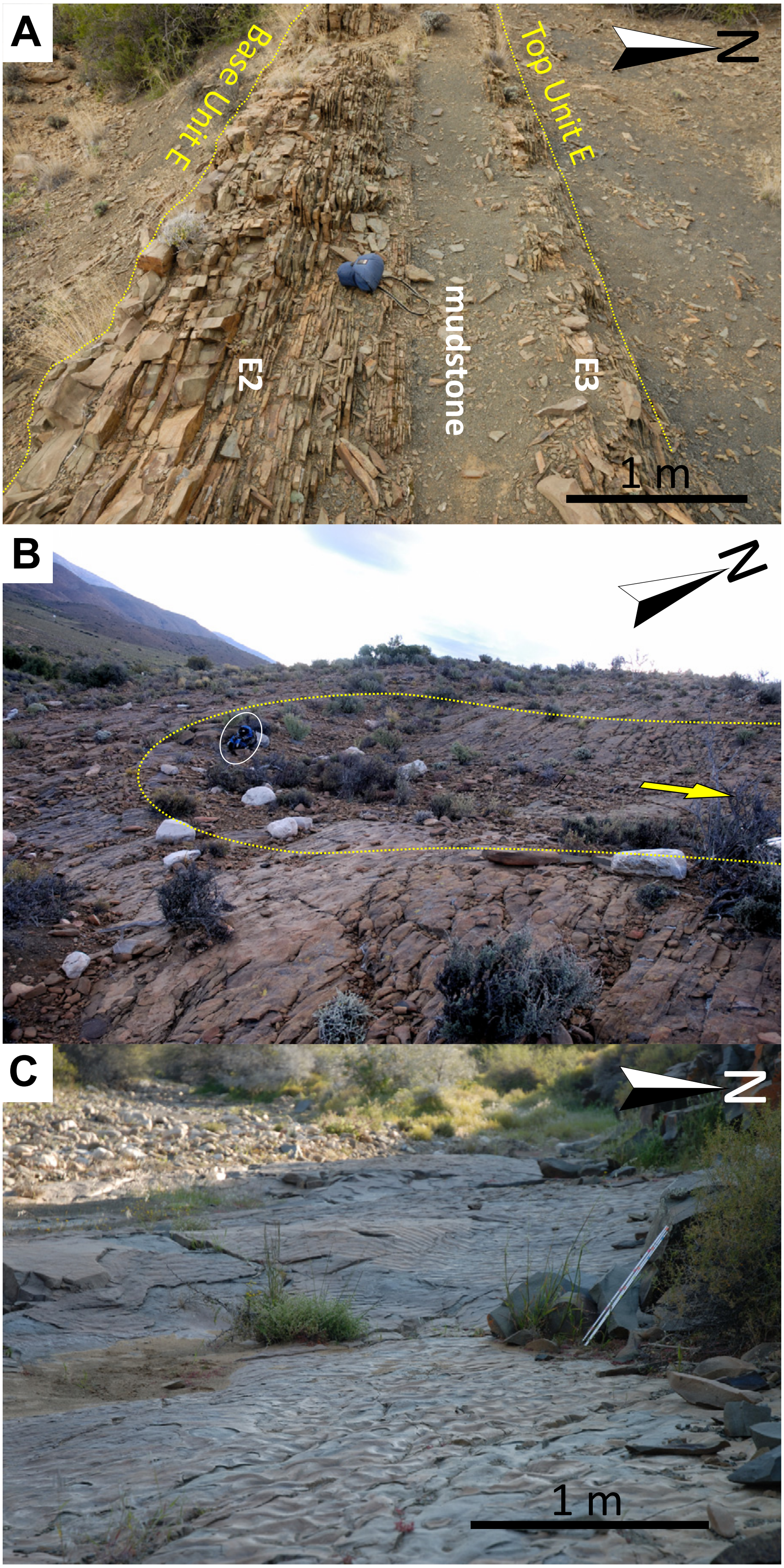

Figure 9. Representative photographs of the characteristics of the interpreted sediment bypass–dominated tract in Unit E (the top surface of E3) in the Floriskraal syncline. (A) The extensive but thin E2 and E3 succession between updip slope channel levees and downdip lobe complexes, characterized by thin-bedded ripple-laminated deposits with multiple scour surfaces. (B, C) The top surfaces of the E3 lowstand systems tract in the sediment bypass–dominated area, including megaflutes (edge marked by yellow dotted line, arrow marks paleoflow direction), mudstone rip-up clast horizons, and remobilized sediments. Circled object in B is 50-cm-high ruc-sac.

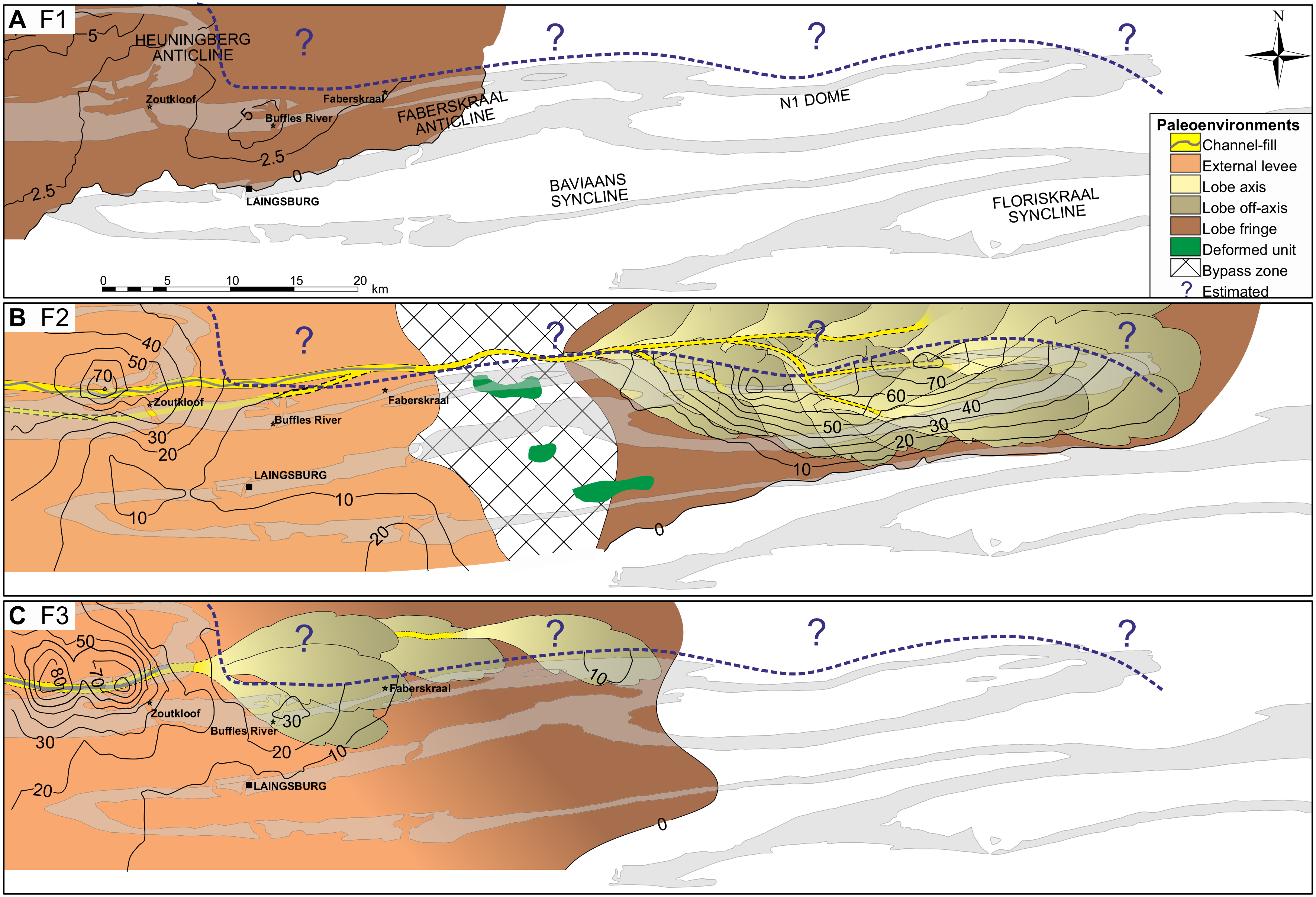

Figure 10. Thickness isopach and gross depositional environment maps for the individual constituent lowstand systems tracts (F1, F2, and F3) of the Unit F lowstand sequence set. Positions of channels are tied to outcrop location, but lobe boundaries are not precise positions. Note the clear progradational trend of successive lowstand systems tracts and the sand- and/or sandstone-detached lobes within F2. Some updip data are from Figueiredo et al. (2010).

F1 Lowstand Systems Tract: Downdip Section

Unit F1 is not developed in the distal parts of the basin, and downlaps out in the central Laingsburg area.

F2 Lowstand Systems Tract: Updip Section

Stratigraphic mapping led to the identification of an ~150-m-deep flat-based F2-aged erosion surface, which cuts out F1, the E–F mudstone, and all of Unit E on the southern flank of the Heuningberg anticline (Fig. 5; Figueiredo et al., 2010, 2013). This is interpreted as an entrenched slope valley that is steep sided and largely filled with thin-bedded siltstones, but with basal remnants of sand-prone channel fills and mud-prone debrites (Fig. 10B). This valley was a major conduit that transported sediment downdip to the east.

F2 Lowstand Systems Tract: Downdip Section

Downdip the valley is interpreted to extend in subcrop through the Zoutkloof syncline or beyond the Heuningberg anticline nose toward the Faberskraal area (Fig. 10B). The external levee deposits adjacent to the entrenched system are interpreted to be genetically related to a precursor channel-levee system prior to the formation of the major valley system. Regional mapping and correlation of F2 shows that it forms a thick levee wedge in the updip section and forms the most regional exposed lowstand systems tract of Unit F to the south and southeast of the depocenter. F2 shows an area of thinning down to 1 m thickness, associated with scouring and deformational features, west of the N1 Dome (Fig. 10B). A few kilometers further downdip, in the N1 Dome area, F2 thickens to more than 100 m of intercalated sand-rich channel-fill and lobe deposits. A series of sand-prone channel fills erode into the E–F mudstone and completely remove Unit E toward the northeast of the N1 Dome.

F3 Lowstand Systems Tract: Updip Section

F3 comprises a slope channel system filled by laterally migrating channels and/or channel complexes and flanked by external levees (Figueiredo et al., 2013; Fig. 10C).

F3 Lowstand Systems Tract: Downdip Section

F3 is interpreted to backstep relative to F2. Frontal lobe deposits in the Buffels River area continue toward the east where they share characteristics with terminal lobes (sensu Prélat et al., 2009) (Fig. 10C).

Map-View Stacking Patterns of Lowstand Systems Tracts

The stacking patterns of individual lowstand systems tracts within lowstand sequence sets can be constrained. Unit C advanced farthest into the basin during the C2 lowstand systems tract, with considerable evidence for sediment bypass at this time at the CD Ridge. A common levee over lobe motif supports a progradational pattern toward the east within C2. C3 shows a backstep of the Unit C system (Morris et al., 2014b). In the Unit D composite sequence, most of the sandstone is in the downdip lobes to the east (Figs. 4 and 5). There are deep incisions in the western updip area, and significant volumes of sand were bypassed, with small amounts present at the base of external levees. Unit D shows a downdip change in proportion of levee to lobe. In the updip quarter of the study area the levee percentage is 80%–100% while downdip it drops to 30%–50% in the N1 Dome and laterally equivalent areas. Approximately 50 km farther downdip and across strike in the Floriskraal area, the lobe percentage reaches 100% (Figs. 7B, 7C). This trend, and the presence of late-stage erosion, suggests a strongly progradational pattern throughout D2, but D3 marks the overall backstep of the systems with vertical channel aggradation and development of internal levees (Hodgson et al., 2011). Internally, Unit E shows a progradational trend and also steps farther into the basin across thick lobe complexes in Units C and D. The updip area of Unit E shows multiple channel deposits across the CD Ridge, N1 Dome, and Zoutkloof and Floriskraal syncline areas (Fig. 8B). Unit E is thin (<20 m thick) between the Floriskraal and Faberskraal synclines and consists of thin-bedded siltstone facies. For Unit F, the overall stratigraphic organization of the lowstand sequence set indicates two stages of basinward stepping of the depositional system followed by a third retreating stage (Fig. 10A–10C). An area of thin and thin-bedded stratigraphy similar to Unit E separates the channel-levee systems and the sand-prone lobes. In summary, lowstand sequence sets show an organized stacking pattern of their component sequences in map view, based on mapping of throughgoing mudstones. Units C, D, and F all indicate a basinward then landward stacking pattern, which implies a progradational-aggradational-retrogradational trend in a stratigraphic sucession, a pattern recognized by Flint et al. (2011). A retrogradational phase in Unit E has not been recognized.

DISCUSSION

Stacking Patterns of Lowstand Sequence Sets

Compensational stacking as an autogenic response to relief generated by older deposits is well documented at the scale of individual lobes and their constituent lobe elements, at outcrop (Mutti and Sonnino, 1981; Prélat et al., 2009; Prélat and Hodgson, 2013), in the subsurface (Deptuck et al., 2007; Jegou et al., 2008), and through numerical modeling studies (Pyrcz et al., 2005; Straub et al., 2009; Groenenberg et al., 2010). This style of stacking has also been documented at the scale of lowstand systems tract (lobe complex sets) in Unit C (Di Celma et al., 2011) and in other deep-water systems (e.g., Jennette et al., 2000; Dmitrieva et al., 2012). Here we investigate whether compensational stacking is present in the linked slope–basin-floor systems of Units C–F.

The isopach thickness maps and paleoenvironmental reconstructions have been combined into maps to help identify stacking patterns at composite sequence and composite sequence set scales within the >2500 km^2 study area (Figs. 11A–11D). On the slope segment, the axes of lowstand sequence sets (C and D, E and F) are marked by the deepest points of erosion, which are referred to as fairways (e.g., Hurst et al., 1999). Lowstand sequence set D is subvertically stacked above lowstand sequence set C, and the same aggradational stacking pattern is observed for E and F (Fig. 12). Control on the subvertical stacking at the scale of the sequence set is likely to be a combination of deep updip entrenchment and external levee confinement that were able to fix the entry point and slope pathway of submarine conduits over extended time periods (Fig. 13). Structural or inherited controls that fixed the entry point cannot be discounted. Differential compaction above the Unit C and D composite sequence set was interpreted to have influenced the position of the Unit E and F composite sequence set on the slope (Figueiredo et al., 2010).

In contrast, on the basin floor, each lowstand sequence set is stacked in a compensational pattern, with the thickest part of successive units laterally offset by >10 km (Fig. 12). This indicates that there was a bathymetric expression of the older sequence set on the seabed, probably generated by differential compaction during deposition of the preceding mud-dominated highstand sequence set (Fig. 13). The compensational patterns on the basin floor indicate that inherited or dynamic topography was not a significant control on basin-floor sediment dispersal patterns or stacking patterns. The southward pinchout of C and E indicates the presence of a north-facing lateral slope (Figs. 6 and 8). The absence of Unit F in the Baviaans South and Floriskraal syncline areas may also reflect the effect of underlying relief on Unit E toward the south and southeast (Fig. 10B). This study extends the range of scales across which compensational stacking is demonstrated at outcrop, to lowstand systems tracts, sequence sets, and composite sequences.

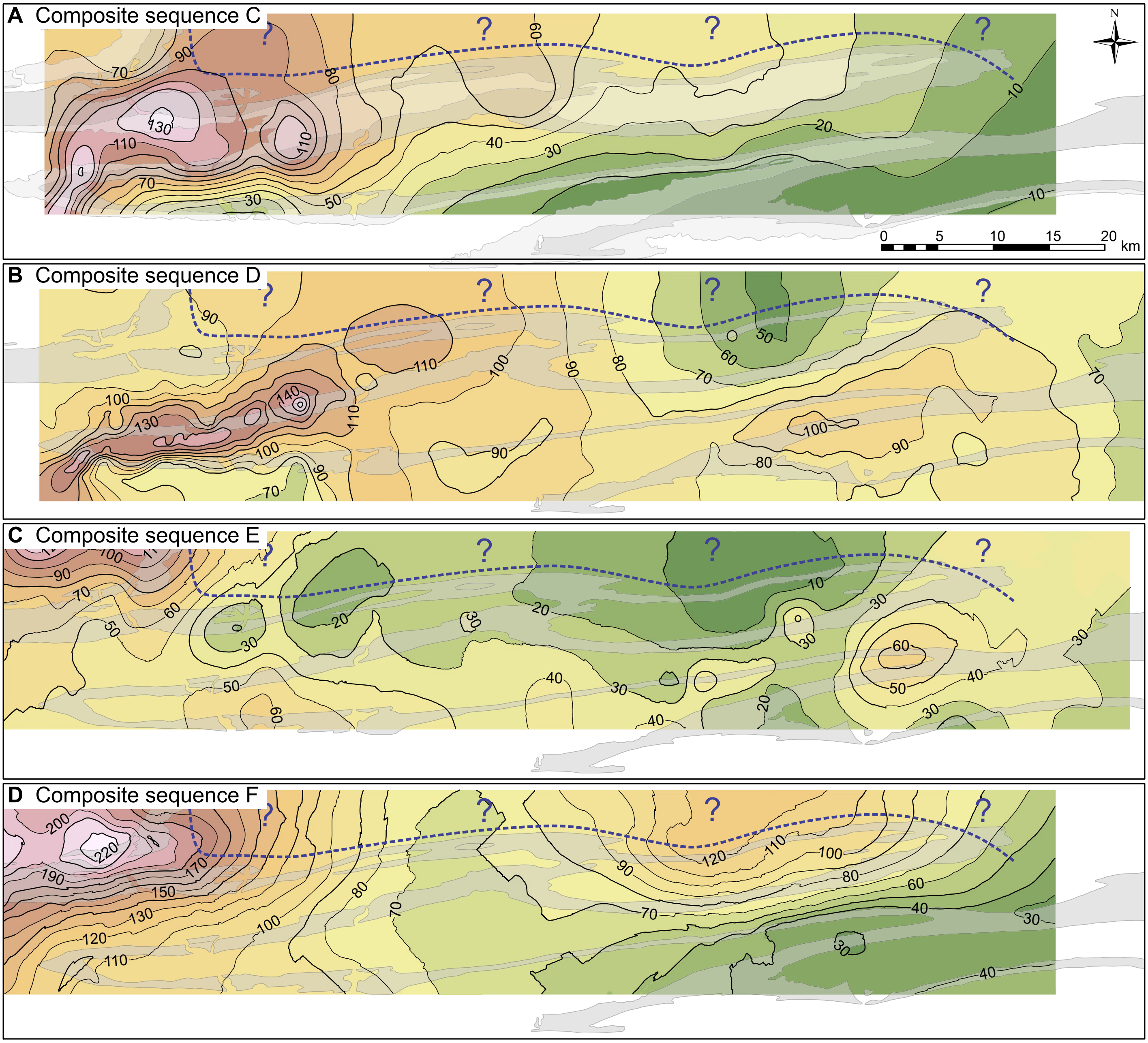

Figure 11. Lowstand sequence set sandstones and transgressive/highstand sequence set mudstones have been combined into maps showing stacking patterns for the four composite sequences. Thin areas are indicated by cold colors (greens) and thick areas with warm colors (pinks). Contours are in meters. Dashed line with question marks indicates area beyond outcrop control.

Identifying the Stratigraphic CLTZ

The CLTZ represents the region that separates well-defined channels or channel-fill deposits from well-defined lobes or lobe facies (Mutti and Normark, 1987), commonly coincident with the base of slope (Wynn et al., 2002). Modern examples provide time slices of erosional and depositional bedforms in the CLTZ. The architectural expression of ancient stratigraphic successions containing deposits and surfaces interpreted as containing the CLTZ commonly have a lack of paleogeographic context. The extensive database presented here provides information on the evolution and migration of the CLTZ. The stacking of external levee deposits over lobe deposits, indicative of system progradation where channels and channel related facies build outward over their own frontal lobe deposits (Brunt et al., 2013a), features strongly in Units C and D (Fig. 5). The extent of progradation, from the most updip basin-floor lobe deposits to the most distal overlying levee deposits, ranges from 60 to 70 km in Units C and D. This architecture cannot represent movement of the geomorphic slope by an equivalent amount; however, it may reflect the increasing efficiency and momentum of flows reaching the basin floor, which promotes basinward movement of the CLTZ. In contrast, levee deposits are

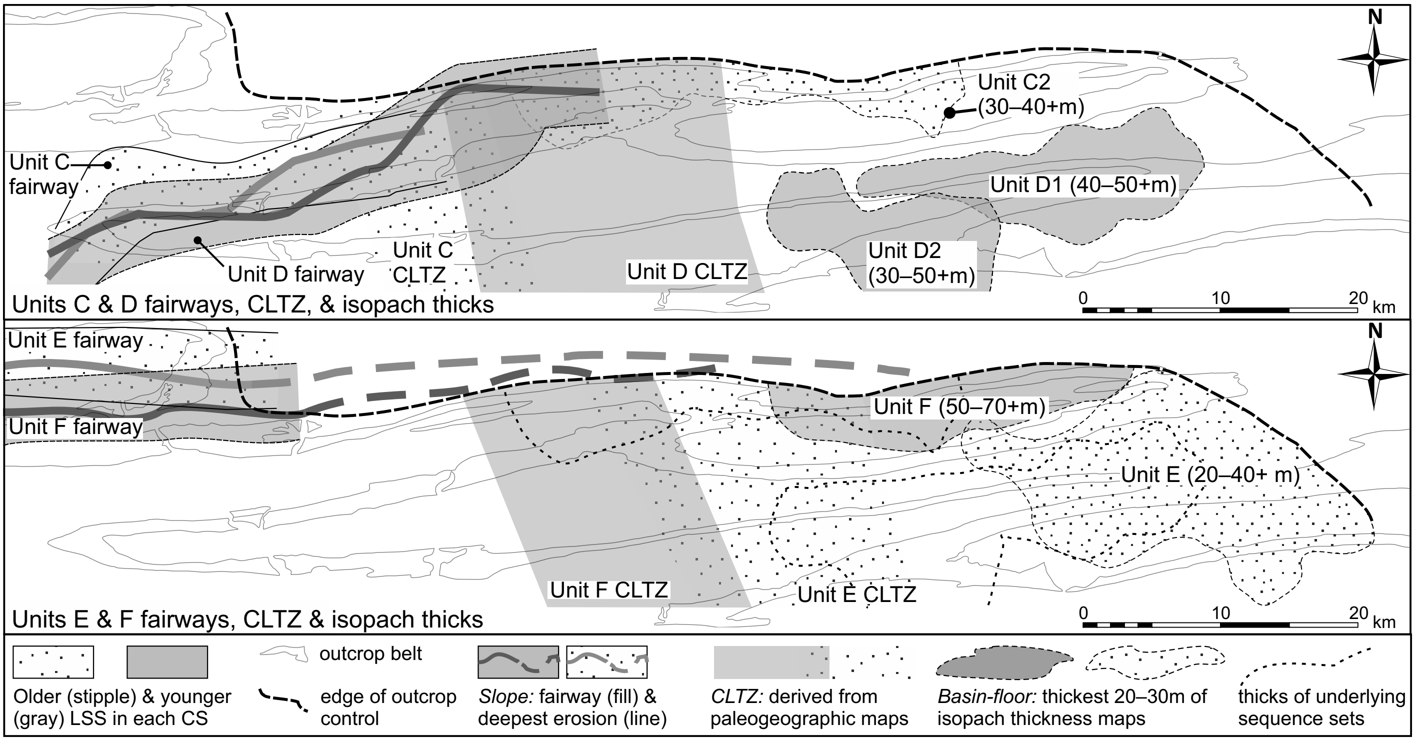

Figure 12. Maps to illustrate the stacking patterns of different components of lowstand sequence sets (LSS) within each of the composite sequences (CS). The older LSS has a stippled fill and the younger is gray. On the slope segment, the major fairways (shaded) and deepest points of erosion (lines) of lowstand sequence sets indicate a subvertical stacking pattern. The channel-lobe transition zone (CLTZ), as defined by gross depositional environment maps, does not migrate basinward as would be expected if the basin margin prograded, but changes character from sandstone-attached (Units C and D) to sandstone-detached (Units E and F). On the basin-floor segment, isopach thickness contours (thicks; thickest = 20–30 m) indicate compensational stacking between lowstand sequence sets. D is subvertically stacked above lowstand sequence set C, and the same stacking pattern is observed for E and F.

largely absent downdip of the interpreted position of the base of slope for Units E and F. The possible controls on the transition from early strongly progradational sand- and/or sandstone-attached fans to late-stage aggradational sand- and/or sandstone-detached fans are discussed in the following section.

Sand- and/or Sandstone-Attached and Detached Systems

Units C and D have been mapped from entrenched slope valleys, interpreted to be on the middle to lower slope, downdip through levee-confined channel systems to attached sand-rich lobe complexes over distances of 50–100 km (Figs. 6 and 7). A general increase in the proportion of sandstone in the fills of channel systems downdip suggests that there is sandstone connectivity between channel fills and lobe deposits, although with a complicated stratigraphic architecture characterized by erosion surfaces, channel-margin thin beds, and channel base lag deposits. Units E and F have been mapped from upper slope entrenched valleys to sand-rich lobe complexes over similar length scales to Units C and D (80 km or more). However, the downdip facies transitions are more complicated. Extensive tracts of sand-poor stratigraphy separate the updip intraslope lobes and levee-confined and entrenched channel systems from thick sand-prone lobe complexes (Figs. 8 and 10). The stratigraphy in these areas is much thinner than updip and downdip, and is characterized by thin beds. In Unit E, this sand-poor tract is 5–30 km in dip length and widens to the north, and is >20 km in along-slope width. In Unit F, the spatially coincident sand-poor tract is 15 km in dip length and >20 km in width (Figs. 5 and 12). Therefore, Units E and F are classed as sand- and/or sandstone-detached systems where, at the scale of the study area, there is unlikely to be physical sandstone continuity between updip channel fills and downdip lobes.

There are two explanations for the presence of these tracts of thin, sand-poor stratigraphy: (1) the sand-prone lobe deposits downdip are supplied by major conduits outside the study area, or (2) this area represents a zone of long-term sand bypass. The facies associations preserved in these sand-poor areas comprise thin-bedded and ripple laminated deposits, typical of distal levee fringes. However, multiple scour surfaces are present, and the top surfaces of lowstand systems tracts include assemblages of megaflutes, mudstone rip-up clast horizons, soft-sediment deformed units that preserve evidence of downslope shear, and thin-bedded traction-dominated sandstones (Fig. 9). The paleocurrents from the sand-poor tracts are aligned with those recorded in updip channel levees and downdip lobes. We interpret the facies association and paleocurrent directions recorded in the sand-poor tract to represent a high-energy erosional sand-bypass environment. Similar thin but high-energy surfaces have been identified in clinothems from the Tres Pasos Formation of the Magallanes Basin, Chile (Hubbard et al., 2010); however, in that system the bypass surface is on the slope of a basin-margin–scale clinoform and does not separate sand-rich parts of the system.

Possible reasons for the development of the sand-detached systems are (1) a change in incoming flow characteristics that results in sand

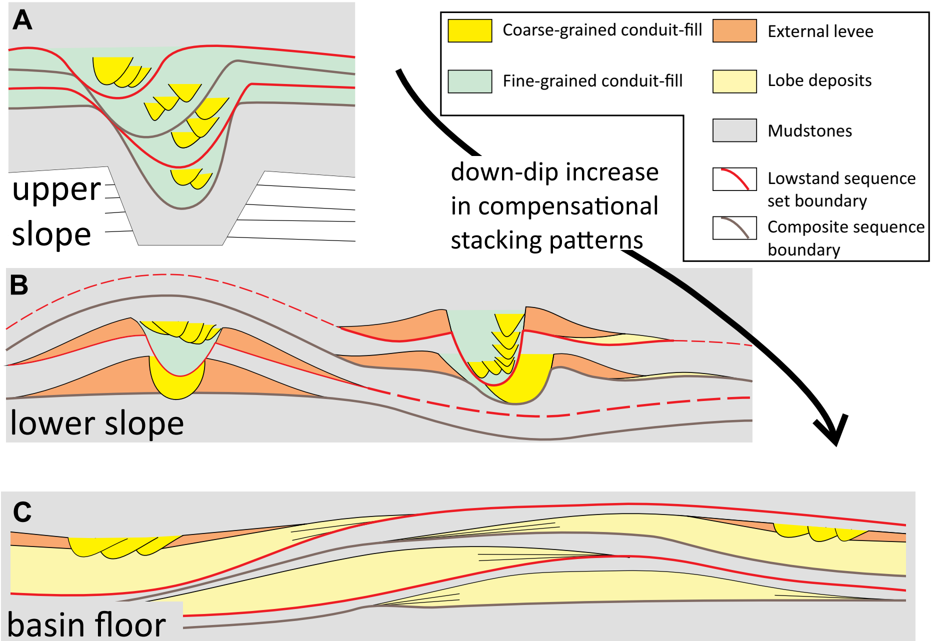

Figure 13. Observed stacking patterns at sequence set, composite sequence, and composite sequence set scales from upper slope to basin floor (>100 km dip length) in the Laingsburg depocenter. The amount of offset attributed to compensational stacking is partly controlled by degree of confinement, which decreases down system. Brown lines are composite sequence boundaries, and red lines are lowstand sequence set boundaries. (A) Upper slope: aggradational stacking of sequences, composite sequences, and sequence sets. (B) Lower slope: aggradational stacking of sequences and sequence sets and compensational stacking of composite sequence sets. (C) Basin floor: compensational stacking of sequences and composite sequences.

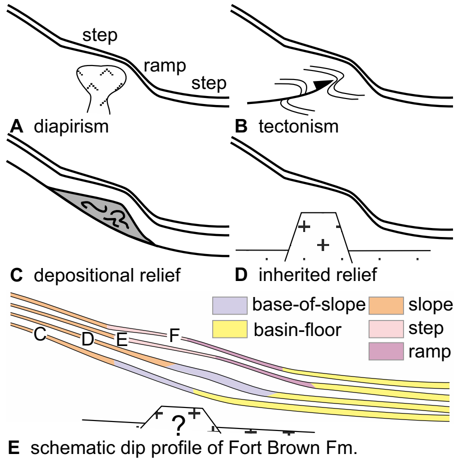

Figure 14. (A–D) Illustrations of a step-ramp-step morphology of a slope and some of the different mechanisms that can be invoked to explain the presence of stepped slope profiles. (E) Dip-oriented slope profiles for Units C–F (Fort Brown Formation). These are not accurate geometric reconstructions, but attempt to show the stacking patterns and changes in slope profile interpreted from facies distributions and thicknesses of composite sequences across the study area.

bypass across discrete surfaces, (2) a change in flow confinement so that flows are able to increase in momentum and deposit farther into the basin, or (3) a local increase in gradient on a stepped profile where the sand bypass zone is a high-gradient ramp between steps (Fig. 14).

One explanation for the development of sand- and/or sandstone-detached systems is that the characteristics of the incoming flows, such as their magnitude and grain size, changed such that the Unit E and F systems were not in equilibrium for a period (Kneller 2003), and changed from depositional to erosional. However, this explanation would require discrete periods during the Unit E and F sediment supply when incoming flows changed, but not in Units C and D. This explanation does not account for the presence of an intraslope lobe updip, or the fact that terminal lobe deposits in Units E and F share close affinities in thickness, grain size, and stacking patterns with Units C and D. Furthermore, the position of the base-of-slope area, as defined by a change in the dominant architectural elements from channel levee–dominated to lobe-dominated deposits, does not move much through time (Fig. 12). The locations of the sand-poor tracts in Units E and F are spatially similar (Fig. 12), and in an area where underlying Unit D is also thin (Figs. 7 and 12), suggesting an intrinsic control in the development of the sand- and/or sandstone-detached systems.

The tracts dominated by sand bypass in Units E and F may have developed due to increased confinement of the flows. A modern example is the Agadir system, offshore Morocco, where a very slight change in basin-floor gradient and confinement has led to a long-term change in flow process behavior and intrasystem sediment bypass (Stevenson et al., 2012). In addition, we cannot discount the existence of mud- and silt-filled channel systems present in the sand-poor tracts that may have developed, but these features are difficult to identify at outcrop due to their fine-grained fill. However, this does not explain the presence of intraslope lobe deposits and the thinness of Units E and F (Fig. 5). Alternatively, local compressional tectonics could have led to increased flow confinement, although no structure has been identified that could be responsible for such a discrete tract of sand bypass.

An alternative explanation for successive units to be thinner in the same part of the basin and for the facies to indicate higher energy and more sand bypass is that an area with less accommodation and/or steeper slopes developed. Downslope changes in accommodation are supported by the presence of perched, or intraslope, lobe deposits and the thin accumulation of Units E and F (Figs. 5, 8, and 10). The large-scale architecture is consistent with the development of a stepped slope profile. Step flats are areas of net accumulation and have a low or a negative gradient, whereas ramps are zones of net sediment bypass (Fig. 14). Basin margins with a stepped profile during deposition have a major influence on sediment dispersal patterns and alternating sections of erosion and bypass (Meckel et al., 2002; O'Byrne et al., 2004; Smith, 2004; Gamberi and Rovere, 2011; Bohn et al., 2012; Hay, 2012; Prather et al., 2012).

Mechanisms invoked to explain changes in downslope gradient, and the development of a stepped profile, include dynamic substrates (e.g., Prather et al., 1998; Mayall et al., 2006; Clark and Cartwright, 2009; Hay, 2012; Oluboyo et al., 2014), depositional relief (e.g., Posamentier and Walker, 2006), inherited bathymetry (e.g., Adeogba et al., 2005; Olafiranye et al., 2013), and differential compaction (e.g., Koša, 2007) (Fig. 14). In this instance the ramp would have been northeast facing, consistent with the overall paleocurrent direction of the underlying (Sixsmith et al., 2004; Di Celma et al., 2011) and overlying (Jones et al., 2013) stratigraphy. We emphasize that the changes in gradient are likely to have been very slight, and are difficult to constrain from outcrop data. A dynamic substrate above salt or mud diapirism is not supported because there is no salt in the basin fill, and the mudstones between lowstand sequence sets thin gradually basinward. Depositional relief is not considered a major driving mechanism because there are no large mass transport deposits. A local increase in gradient could be attributed to tectonic tilting or blind thrust propagation into the basin. Synsedimentary faulting and folding have a significant impact on sediment dispersal patterns in deep-water settings (e.g., Hodgson and Haughton 2004; Kane et al., 2010). If there was an active tectonic structure responsible for locally steepening the slope to the northeast during sedimentation, it was at a high angle to the later fold structures, and there is no evidence that it propagated to the surface. Differential compaction over the underlying composite sequence set may have led to a local increase in gradient on the seabed that promoted a local and persistent increase in flow energy and sand bypass. However, Units C and D are not thicker in the area where Units E and F thin. An alternative way that differential compaction may have led to the development of a northeast-facing ramp is that there is a deeper inherited structure. The presence of rigid structures that formed during synrift tectonics can maintain a seabed expression for millions of years through differential compaction (e.g., Færseth and Lien, 2002) (Fig. 14). Further work using gravity and magnetic data is needed to investigate the role of inherited structures on the physiography of the younger basin fill. However, northwest-striking rift basins that developed during the early Paleozoic provide one mechanism to generate a heterogeneous basement configuration (e.g., Tankard et al., 2009).

CONCLUSIONS

The continuity and spatial distribution of the Laingsburg Karoo outcrop data set has allowed the depositional architecture of four successive composite sequences to be reconstructed from slope channel levees to basin-floor fans over a 2500 km^2 area. The geographic and stratigraphic constraints of this unique data set confirm widely employed models that predict that the percentage of sand will increase from the slope to the proximal basin floor, and that slope channels are agents of sediment bypass. A stacking pattern common to the Units C, D, and F lowstand sequence sets is basinward then landward stepping. This pattern could be attributed to allogenic controls, such as relative base level, tectonics, and/or climate, influencing the waxing then waning of sediment supply to the deep water. Establishing the role of autogenic controls on the depositional architectural of deep-water systems is more challenging. We note that external levee deposits overlie lobe deposits within the sand- and/or sandstone-attached lowstand systems tracts. The depositional relief of frontal lobes can help to establish external levees (Morris et al., 2014b). An increase in flow confinement provides a mechanism to help propagate channels farther into the basin. Furthermore, compensational stacking has been demonstrated to occur at the scale of composite sequences. Thus at sequence through to composite sequence set scale, sediment dispersal patterns and depositional architecture are controlled by both the interplay between autogenic responses to depositional relief and gradient changes and allogenic modulation of sediment supply to the deep-water slope and basin floor.

This unique outcrop data set provides exploration-scale insights and understanding into how different segments of a prograding slope evolved over time in terms of gradient, morphology, and hence the degree to which sand was stored or bypassed to the basin floor. For the first time, sand-detached submarine lobe complexes have been identified in a system-scale context at outcrop, with CLTZs of markedly different stratigraphic architecture to sand-attached systems. The stratigraphic evolution of composite sequences from sand-attached to sand-detached systems is interpreted to reflect the development of a stepped slope profile. The exact mechanism that established the stepped profile is not clear, although we suspect the role of differential subsidence over inherited basement structures may have developed a stepped profile and initiated sand bypass. Mutti and Ricci Lucchi (1975) advocated detachment of lobes from their associated feeder channels as a result of sediment bypass; they speculated that if sediment bypass persisted for a considerable length of time, a relatively thick zone of mudrock would develop that separated channel mouth deposits from lobe deposits. In a subsurface scenario this lithological break could act as a permeability barrier between sand-rich lobes and updip reservoir facies. Detached lobes could therefore represent updip stratigraphic traps in the subsurface. In reflection seismic data sets a physical connection might be imaged, although the degree of reservoir connectivity, and the potential for stratigraphic traps, might be less clear.

ACKNOWLEDGMENTS

The work presented here is part of the SLOPE Project, phase 3. We thank the consortium of oil company sponsors for both technical input and financial support (Anadarko, BHP Billiton, BP, Chevron, ConocoPhillips, E.ON, ExxonMobil, Gaz de France-Suez, Maersk, Murphy, Petrobras, Schlumberger, Shell, Statoil, Total, Tullow, VNG Norge, and Woodside). This manuscript has benefited from thorough and constructive reviews by Zane Jobe, Christian Carvajal, and an anonymous reviewer, and Thematic Set Editor Andrea Fildani. We thank many colleagues for field work assistance, notably John Kavanagh, Laura Fielding, and Ashley Clark. De Ville Wickens was a major help in project organization and management. We also thank the numerous landowners for their kind permission to work on many farms throughout the southwest Karoo.

REFERENCES CITED

Abreu, V., Sullivan, M., Pirmez, C., and Mohrig, D., 2003, Lateral accretion packages (LAPs): An important reservoir element in deep water sinuous channels: Marine and Petroleum Geology, v. 20, p. 631–648, doi:10.1016/j.marpetgeo.2003.08.003.

Adeogba, A.A., McHargue, T.R., and Graham, S.A., 2005, Transient fan architecture and depositional controls from near-surface 3-D seismic data, Niger Delta continental slope: American Association of Petroleum Geologists Bulletin, v. 89, p. 627–643, doi:10.1306/11200404025.

Amy, L.A., and Talling, P.J., 2006, Anatomy of turbidites and linked debrites based on long distance (120 × 30 km) bed correlation, Marnoso Arenacea Formation, Northern Apennines, Italy: Sedimentology, v. 53, p. 161–212, doi:10.1111/j.1365-3091.2005.00756.x.

Armitage, D.A., McHargue, T., Fildani, A., and Graham, S.A., 2012, Post avulsion channel evolution: Niger Delta continental slope: American Association of Petroleum Geologists Bulletin, v. 96, p. 823–843, doi:10.1306/09131110189.

Beauboeuf, R.T., Rossen, C., Zelt, F.B., Sullivan, M.D., Mohrig, D.C., and Jennette, D.C., 2000, Deep-water sandstones, Brushy Canyon Formation, west Texas: American Association of Petroleum Geologists Continuing Education Course Notes 40, 50 p.

Bernhardt, A., Jobe, Z.R., and Lowe, R., 2011, Stratigraphic evolution of a submarine channel-lobe complex system in a narrow fairway within the Magallanes Foreland Basin, Cerro Toro Formation, southern Chile: Marine and Petroleum Geology, v. 28, p. 785–806, doi:10.1016/j.marpetgeo.2010.05.013.

Bohn, C.W., Flemings, P.B., and Slingerland, R.L., 2012, Accommodation change during bypass across a late-stage fan in the shallow Auger basin, *in* Prather, B.E., et al., eds., Application of the principles of seismic geomorphology to continental-slope and base-of-slope systems: Case studies from seafloor and near-seafloor analogues: SEPM (Society for Sedimentary Geology) Special Publication 99, p. 225–242, doi:10.2110/pec.12.99.0225.

Brunt, R.L., Di Celma, C.N., Hodgson, D.M., Flint, S.S., Kavanagh, J.P., and van der Merwe, W.C., 2013a, Driving a channel through a levee when the levee is high: An outcrop example of submarine down-dip entrenchment: Marine and Petroleum Geology, v. 41, p. 134–145, doi:10.1016/j.marpetgeo.2012.02.016.

Brunt, R.L., Hodgson, D.M., Flint, S.S., Pringle, J.K., Di Celma, C., Prélat, A., and Grecula, M., 2013b, Confined to unconfined: Anatomy of a base of slope succession, Karoo Basin, South Africa: Marine and Petroleum Geology, v. 41, p. 206–221, doi:10.1016/j.marpetgeo.2012.02.007.

Burgreen, B., and Graham, S., 2014, Evolution of a deep-water lobe system in the Neogene trench-slope setting of the East Coast Basin, New Zealand: Lobe stratigraphy and architecture in a weakly confined basin configuration: Marine and Petroleum Geology, v. 54, p. 1–22, doi:10.1016/j.marpetgeo.2014.02.011.

Catterall, V., Redfern, J., Gawthorpe, R.L., Hensen, D., and Thomas, M., 2010, Architectural style and quantification of a submarine channel-levee system located in a structurally complex area: Offshore Nile delta: Journal of Sedimentary Research, v. 80, p. 991–1017, doi:10.2110/jsr.2010.084.

Chapin, M.A., Davies, P., Gibson, J.L., and Pettingill, H.S., 1994, Reservoir architecture of turbidite sheet sandstones in laterally extensive outcrops, Ross Formation, western Ireland, *in* Weimer, P., et al., eds., Submarine fans and turbidite systems: Sequence stratigraphy, reservoir architecture and production characteristics, Gulf of Mexico and international: GCSSEPM (Gulf Coast Section, Society for Sedimentary Geology) Foundation 15th Annual Research Conference Proceedings, p. 53–68.

Clark, I.R., and Cartwright, J.A., 2009, Interactions between submarine channel systems and deformation in deepwater fold belts: Examples from the Levant Basin, Eastern Mediterranean sea: Marine and Petroleum Geology, v. 26, p. 1465–1482, doi:10.1016/j.marpetgeo.2009.05.004.

Deptuck, M.E., Sylvester, Z., Pirmez, C., and O'Byrne, C., 2007, Migration, aggradation history and 3-D seismic geomorphology of submarine channels in the Pleistocene Benin-major Canyon, western Niger Delta slope: Marine and Petroleum Geology, v. 24, p. 406–433, doi:10.1016/j.marpetgeo.2007.01.005.

Di Celma, C., Brunt, R.L., Hodgson, D.M., Flint, S.S., and Kavanagh, J.P., 2011, Spatial and temporal evolution of a Permian submarine slope channel-levee system, Karoo Basin, South Africa: Journal of Sedimentary Research, v. 81, p. 579–599, doi:10.2110/jsr.2011.49.

Dmitrieva, E., Jackson, C.A.-L., Huuse, M., and McCarthy, A., 2012, Paleocene deep-water depositional systems in the North Sea basin: A 3D seismic and well data case study, offshore Norway: Petroleum Geoscience, v. 18, p. 97–114, doi:10.1144/1354-079311-027.

Eschard, R., Albouya, E., Deschamps, R., Euzena, T., and Ayub, A., 2003, Downstream evolution of turbiditic channel complexes in the Pab Range outcrops (Maastrichtian, Pakistan): Marine and Petroleum Geology, v. 20, p. 691–710, doi:10.1016/j.marpetgeo.2003.02.004.

Færseth, R.B., and Lien, T., 2002, Cretaceous evolution in the Norwegian Sea—A period characterized by tectonic quiescence: Marine and Petroleum Geology, v. 19, p. 1005–1027, doi:10.1016/S0264-8172(02)00112-5.

Figueiredo, J., Hodgson, D.M., and Flint, S.S., 2010, Depositional environments and sequence stratigraphy of an exhumed Permian mud-dominated submarine slope succession, Karoo basin, South Africa: Journal of Sedimentary Research, v. 80, p. 97–118, doi:10.2110/jsr.2010.002.

Figueiredo, J.J.P., Hodgson, D.M., Flint, S.S., and Kavanagh, J.P., 2013, Architecture of a channel complex formed and filled during long-term degradation and entrenchment on the upper submarine slope, Unit F, Fort Brown Fm., SW Karoo Basin, South Africa: Marine and Petroleum Geology, v. 41, p. 104–116, doi:10.1016/j.marpetgeo.2012.02.006.

Fildani, A., and Normark, W.R., 2004, Late Quaternary evolution of channel and lobe complexes of Monterey Fan: Marine Geology, v. 206, p. 199–223, doi:10.1016/j.margeo.2004.03.001.

Fildani, A., Weislogel, A., Drinkwater, N.J., McHargue, T., Tankard, A., Wooden, J., Hodgson, D.M., and Flint, S., 2009, U-Pb zircon ages from the southwestern Karoo basin, South Africa—Implications for the Permian-Triassic boundary: Geology, v. 37, p. 719–722, doi:10.1130/G25685A.1.

Flint, S.S., Hodgson, D.M., Sprague, A., Brunt, R.L., Box, D., Van Der Merwe, W.C., Figueiredo, J., Di Celma, C., Prélat, A., and Kavanagh, J.P., 2011, Depositional architecture and sequence stratigraphy of the Karoo basin floor to shelf edge succession, Laingsburg depocentre, South Africa: Marine and Petroleum Geology, v. 28, p. 658–674, doi:10.1016/j.marpetgeo.2010.06.008.

Fonnesu, F., 2003, 3D seismic images of a low-sinuosity slope channel and related depositional lobe (West Africa deep-offshore): Marine and Petroleum Geology, v. 20, p. 615–629, doi:10.1016/j.marpetgeo.2003.03.006.

Fugelli, E.M.G., and Olsen, T.R., 2005a, Screening for deep-marine reservoirs in frontier basins: Part 1—Examples from offshore mid-Norway: American Association of Petroleum Geologists Bulletin, v. 89, p. 853–882, doi:10.1306/02110504029.

Fugelli, E.M.G., and Olsen, T.R., 2005b, Risk assessment and play fairway analysis in frontier basins: Part 2—Examples from offshore mid-Norway: American Association of Petroleum Geologists Bulletin, v. 89, p. 883–896, doi:10.1306/02110504030.

Gamberi, F., and Rovere, M., 2011, Architecture of a modern transient fan (Villafranca fan, Gioia basin–Southeastern Tyrrhenian Sea): Sedimentary Geology, v. 236, p. 211–225, doi:10.1016/j.sedgeo.2011.01.007.

Gardner, M.H., and Borer, J., 2000, Submarine channel architecture along a slope to basin profile, Permian Brushy Canyon Formation, west Texas, *in* Bouma, A.H., et al., eds., Fine-grained turbidite systems: American Association of Petroleum Geologists Memoir 72 and SEPM (Society for Sedimentary Geology) Special Publication 68, p. 195–215.

Gardner, M.H., Borer, J.M., Melick, J.J., Mavilla, N., Dechesne, M., and Wagerle, R.N., 2003, Stratigraphic process-response model for submarine channels and related features from studies of Permian Brushy Canyon outcrops, west Texas: Marine and Petroleum Geology, v. 20, p. 757–787, doi:10.1016/j.marpetgeo.2003.07.004.

Grecula, M., Flint, S.S., Wickens, H.D., and Johnson, S.D., 2003, Upward-thickening patterns and lateral continuity of Permian sand-rich turbidite channel fills, Laingsburg Karoo, South Africa: Sedimentology, v. 50, p. 831–853, doi:10.1046/j.1365-3091.2003.00576.x.

Groenenberg, R.M., Hodgson, D.M., Prélat, A., Luthi, S.M., and Flint, S., 2010, Autogenic controls on the geometry and stacking pattern of terminal lobe deposits in distributive deep-water systems: Integrating outcrop observations and process-based numerical model realizations: Journal of Sedimentary Research, v. 80, p. 252–267, doi:10.2110/jsr.2010.028.

Hay, D., 2012, Stratigraphic evolution of a tortuous corridor from the stepped slope of Angola, *in* Prather, B.E., et al., eds., Application of the principles of seismic geomorphology to continental-slope and base-of-slope systems: Case studies from seafloor and near-seafloor analogues: SEPM (Society for Sedimentary Geology) Special Publication 99, p. 163–180, doi:10.2110/pec.12.99.0163.

Hesse, R., 1974, Long-distance continuity of turbidites: Possible evidence for an early Cretaceous trench-abyssal plain in the East Alps: Geological Society of America Bulletin, v. 85, p. 859–870, doi:10.1130/0016-7606(1974)85<859:LCOTPE>2.0.CO;2.

Hodgson, D.M., 2009, Origin and distribution of bipartite beds in sand-rich submarine fans: Constraints from the Tanqua depocentre, Karoo Basin, South Africa: Marine and Petroleum Geology, v. 26, p. 1940–1956, doi:10.1016/j.marpetgeo.2009.02.011.

Hodgson, D.M., and Haughton, P.D.W., 2004, Impact of syn-depositional faulting on gravity current behaviour and deep-water stratigraphy: Tabernas-Sorbas Basin, SE Spain, *in* Lomas, S.A., and Joseph, P., eds., Confined turbidite systems: Geological Society of London Special Publication 222, p. 135–158, doi:10.1144/GSL.SP.2004.222.01.08.

Hodgson, D.M., Di Celma, C., Brunt, R.L., and Flint, S.S., 2011, Submarine slope degradation and aggradation and the stratigraphic evolution of channel-levee systems: Geological Society of London Journal, v. 168, p. 625–628, doi:10.1144/0016-76492010-177.

Hubbard, S.M., Fildani, A., Romans, B.W., Covault, J.A., and McHargue, T.R., 2010, High-relief slope clinoform development: Insights from outcrop, Magallanes Basin, Chile: Journal of Sedimentary Research, v. 80, p. 357–375, doi:10.2110/jsr.2010.042.

Hurst, A., Verstralen, I., Cronin, B., and Hartley, A., 1999, Sand-rich fairways in deep-water clastic reservoirs: Genetic Units, capturing uncertainty, and a new approach to reservoir modeling: American Association of Petroleum Geologists Bulletin, v. 83, p. 1096–1118.

Jackson, C.A.-L., Barber, G.P., and Martinsen, O.J., 2008, Submarine slope morphology as a control on the development of sand-rich turbidite depositional systems: 3D seismic analysis of the Kyrre Fm (Upper Cretaceous), Måløy Slope, offshore Norway: Marine and Petroleum Geology, v. 25, p. 663–680, doi:10.1016/j.marpetgeo.2007.12.007.

Jegou, I., Savoye, B., Pirmez, C., and Droz, L., 2008, Channel–mouth lobe complex of the recent Amazon Fan: The missing piece: Marine Geology, v. 252, p. 62–77, doi:10.1016/j.margeo.2008.03.004.

Jennette, D.C., Garfield, T.R., Mohrig, D.C., and Cayley, G.T., 2000, The interaction of shelf accommodation, sediment supply and sea level in controlling the facies, architecture and sequence stacking patterns of the Tay and Forties/Sele basin-floor fans, central North Sea, *in* Weimer, P., et al., eds., Deep-water reservoirs of the world: GCSSEPM (Gulf Coast Section, Society for Sedimentary Geology) Foundation 20th Annual Bob F. Perkins Research Conference Proceedings, p. 402–421.

Jobe, Z.R., Lowe, D.R., and Morris, W.R., 2012, Climbing-ripple successions in turbidite systems: Depositional environments, sedimentation rates and accumulation times: Sedimentology, v. 59, p. 867–898, doi:10.1111/j.1365-3091.2011.01283.x.

Johnson, S.D., Flint, S., Hinds, D., and Wickens, H.D., 2001, Anatomy of basin floor to slope turbidite systems, Tanqua Karoo, South Africa: Sedimentology, sequence stratigraphy and implications for subsurface prediction: Sedimentology, v. 48, p. 987–1023, doi:10.1046/j.1365-3091.2001.00405.x.

Jones, G.E., Hodgson, D.M., and Flint, S.S., 2013, Contrast in the process response of stacked clinothems to the shelf-slope rollover: Geosphere, v. 9, p. 299–316, doi:10.1130/GES00796.1.

Kane, I.A., and Hodgson, D.M., 2011, Sedimentological criteria to differentiate submarine levee subenvironments: Exhumed examples from the Rosario Fm. (Upper Cretaceous) of Baja California, Mexico, and the Fort Brown Fm. (Permian), Karoo Basin, S. Africa: Marine and Petroleum Geology, v. 28, p. 807–823, doi:10.1016/j.marpetgeo.2010.05.009.

Kane, I.A., Kneller, B.C., Dykstra, M., Kassem, A., and McCaffrey, W.D., 2007, Anatomy of a submarine channel-levee: An example from Upper Cretaceous slope sediments, Rosario Formation, Baja California, Mexico: Marine and Petroleum Geology, v. 24, p. 540–563, doi:10.1016/j.marpetgeo.2007.01.003.

Kane, I.A., Catterall, V., McCaffrey, W.D., and Martinsen, O.J., 2010, Submarine channel response to intrabasinal tectonics: The influence of lateral tilt: American Association of Petroleum Geologists Bulletin, v. 94, p. 189–219, doi:10.1306/08180909059.

Kneller, B.C., 2003, The influence of flow parameters on turbidite slope channel architecture: Marine and Petroleum Geology, v. 20, p. 901–910, doi:10.1016/j.marpetgeo.2003.03.001.

Koša, E., 2007, Differential subsidence driving the formation of mounded stratigraphy in deep-water sediments: Palaeocene, central North Sea: Marine and Petroleum Geology, v. 24, p. 632–652, doi:10.1016/j.marpetgeo.2007.04.001.

Macdonald, H.A., Wynn, R.B., Huvenne, V.A.I., Peakall, J., Masson, D.G., Weaver, P.P.E., and McPhail, S.D., 2011, New insights into the morphology, fill, and remarkable longevity (>0.2 m.y.) of modern deep-water erosional scours along the northeast Atlantic margin: Geosphere, v. 7, p. 845–867, doi:10.1130/GES00611.1.

Maier, K.L., Fildani, A., Paull, C.K., Graham, S.A., McHargue, T.R., Caress, D.W., and McGann, M., 2011, The elusive character of discontinuous deep-water channels: New insights from Lucia Chica channel system, offshore: California Geology, v. 39, p. 327–330, doi:10.1130/G31589.1.

Mayall, M., Jones, E., and Casey, M., 2006, Turbidite channel reservoirs—Key elements in facies prediction and effective development: Marine and Petroleum Geology, v. 23, p. 821–841, doi:10.1016/j.marpetgeo.2006.08.001.

Meckel, L.D., III, Ugueto, G.A., Lynch, D.H., Hewett, B.M., Bocage, E.J., Winker, C.D., and O'Neill, B.J., 2002, Genetic stratigraphy, stratigraphic architecture, and reservoir stacking patterns of the upper Miocene–lower Pliocene Greater Mars–Ursa intraslope basins, Mississippi Canyon, Gulf of Mexico, *in* Armentrout, J., ed., Sequence stratigraphic models for exploration and production: Evolving methodology, emerging models, and application histories: GCSSEPM (Gulf Coast Section, Society for Sedimentary Geology) Foundation 22nd Annual Bob F. Perkins Research Conference Proceedings, p. 113–147.

Moody, J.D., Pyles, D.R., Clark, J., and Bouroullec, R., 2012, Quantitative outcrop characterization of an analog to weakly confined submarine channel systems: Morillo 1 member, Ainsa Basin, Spain: American Association of Petroleum Geologists Bulletin, v. 96, p. 1813–1841, doi:10.1306/01061211072.

Morris, E.A., Hodgson, D.M., Brunt, R.L., and Flint, S.S., 2014a, Origin, evolution and anatomy of silt-prone submarine external levées: Sedimentology, v. 61, p. 1734–1763, doi:10.1111/sed.12114.

Morris, E.A., Hodgson, D.M., Flint, S.S., Brunt, R.L., Butterworth, P.J., and Verhaeghe, J., 2014b, Sedimentology, stratigraphic architecture and depositional context of submarine frontal lobe complexes: Journal of Sedimentary Research, v. 84, p. 763–780.

Mutti, E., 1985, Systems and their relations to depositional sequences, *in* Zuffa, G.G., ed., Provenance of arenites: Interpreting provenance relations from detrital modes of sandstones: NATO-ASI Series 148: Dordrecht, D. Reidel, p. 65–93.

Mutti, E., and Normark, W.R., 1987, Comparing examples of modern and ancient turbidite systems: Problems and concepts, *in* Leggett, J.K. and Zuffa, G.G., eds., Marine clastic sedimentology: Concepts and case studies: London, Graham and Trotman, p. 1–38, doi:10.1007/978-94-009-3241-8_1.

Mutti, E., and Normark, W.R., 1991, An integrated approach to the study of turbidite systems, *in* Weimer, P., and Link, M.H., eds., Seismic facies and sedimentary processes of submarine fans and turbidite systems: New York, Springer-Verlag, p. 75–106, doi:10.1007/978-1-4684-8276-8_4.

Mutti, E., and Ricci Lucchi, F., 1972, Turbidites of the Northern Apennines: Introduction to facies analysis (English translation by T.H. Nilsen, 1978): International Geology Review, v. 20, p. 125–166, doi:10.1080/00206817809471524.

Mutti, E., and Ricci Lucchi, F., 1975, Turbidite facies and facies associations, *in* Mutti, E., et al., eds., Examples of Turbidite facies and Facies Associations from Selected Formations of the Northern Apennines: 9th International Congress of Sedimentology, Field Trip A-11 Guidebook, p. 21–36.

Mutti, E., and Sonnino, M., 1981, Compensation cycles: A diagnostic feature of turbidite sandstone lobes: International Association of Sedimentologists, 2nd European Regional Meeting, Bologna, Abstracts, p. 120–123.

Newton, A.R., 1992, Thrusting on the northern margin of the Cape Fold Belt, near Laingsburg, *in* de Wit, M.J., and Ransome, I.G.D., eds., Inversion tectonics of the Cape Fold Belt, Karoo and Cretaceous Basins of southern Africa: Rotterdam, A.A. Balkema, p. 193–196.

Normark, W.R., 1970, Growth patterns of deep-sea fans: American Association of Petroleum Geologists Bulletin, v. 54, p. 2170–2195.

Normark, W.R., 1978, Fan valleys, channels, and depositional lobes on modern submarine fans: Characters for recognition of sandy turbidite environments: American Association of Petroleum Geologists Bulletin, v. 62, p. 912–931.

O'Byrne, C.J., Prather, B.E., Steffens, G.S., and Pirmez, C., 2004, Reservoir architectural styles across stepped slope profiles: Implications for exploration, appraisal and development [abs.]: Proceedings, American Association of Petroleum Geologists International Conference, Cancún, Mexico, p. A58.

Olafiranye, K., Jackson, C.A.-L., and Hodgson, D.M., 2013, The role of tectonics and mass-transport complex emplacement on upper slope stratigraphic evolution: A 3D seismic case study from offshore Angola: Marine and Petroleum Geology, v. 44, p. 196–216, doi:10.1016/j.marpetgeo.2013.02.016.

Oluboyo, A.P., Gawthorpe, R.L., Bakke, K., and Hadler-Jacobsen, F., 2014, Salt tectonic controls on deep-water turbidite depositional systems: Miocene, southwestern Lower Congo Basin, offshore Angola: Basin Research, v. 26, p. 597–620, doi:10.1111/bre.12051.

Pickering, K.T., and Corregidor, J., 2005, Mass transport complex and tectonics control on confined basin-floor submarine fans, Middle Eocene, south Spanish Pyrenees, *in* Hodgson, D.M., and Flint, S.S. eds., Submarine slope systems: Process and products: Geological Society of London Special Publication 244, p. 51–74, doi:10.1144/GSL.SP.2005.244.01.04.

Posamentier, H.W., and Kolla, V., 2003, Seismic geomorphology and stratigraphy of depositional elements in deep-water settings: Journal of Sedimentary Research, v. 73, p. 367–388, doi:10.1306/111302730367.

Posamentier, H.W., and Walker, R.G., 2006, Deep-water turbidites and submarine fans, *in* Posamentier, H.W., and Walker, R.G., eds., Facies models revisited: SEPM (Society for Sedimentary Geology) Special Publication 84, p. 399–520, doi:10.2110/pec.06.84.0399.

Prather, B.E., Booth, J.R., Steffens, G.S., and Craig, P.A., 1998, Classification, lithologic calibration, and stratigraphic succession of seismic facies of intraslope basins, deep-water Gulf of Mexico: American Association of Petroleum Geologists Bulletin, v. 82, p. 701–728.

Prather, B.E., Pirmez, C., Sylvester, Z., and Prather, D.S., 2012, Stratigraphic response to evolving geomorphology in a submarine apron perched on the upper Niger Delta slope, *in* Prather, B.E., et al., eds., Application of the principles of seismic geomorphology to continental-slope and base-of-slope systems: Case studies from seafloor and near-seafloor analogues: SEPM (Society for Sedimentary Geology) Special Publication 99, p. 145–161, doi:10.2110/pec.12.99.0145.

Prélat, A., and Hodgson, D.M., 2013, The full range of turbidite bed thickness patterns in submarine lobes: Controls and implications: Geological Society of London Journal, v. 170, p. 209–214, doi:10.1144/jgs2012-056.

Prélat, A., Hodgson, D.M., and Flint, S., 2009, Evolution, architecture and hierarchy of distributary deep-water deposits: A high-resolution outcrop investigation from the Permian Karoo Basin, South Africa: Sedimentology, v. 56, p. 2132–2154, doi:10.1111/j.1365-3091.2009.01073.x.

Pringle, J.K., Brunt, R.L., Hodgson, D.M., and Flint, S.S., 2010, Capturing stratigraphic and sedimentological complexity from submarine channel complex outcrops to digital 3D models, Karoo Basin, South Africa: Petroleum Geoscience, v. 16, p. 307–330, doi:10.1144/1354-079309-028.

Pyrcz, M.J., Catuneanu, O., and Deutsch, C.V., 2005, Stochastic surface-based modeling of turbidite lobes: American Association of Petroleum Geologists Bulletin, v. 89, p. 177–191, doi:10.1306/09220403112.

Remacha, E., and Fernández, L.P., 2003, High-resolution correlation patterns in the turbidite systems of the Hecho Group (South-Central Pyrenees, Spain): Marine and Petroleum Geology, v. 20, p. 711–726, doi:10.1016/j.marpetgeo.2003.09.003.

Saller, A.H., and Dharmasamadhi, I.N., 2012, Controls on the development of valleys, canyons, and unconfined channel levee complexes on the Pleistocene slope of East Kalimantan, Indonesia: Marine and Petroleum Geology, v. 29, p. 15–34, doi:10.1016/j.marpetgeo.2011.09.002.

Saller, A.H., Noah, J.T., Ruzuar, A.P., and Schneider, R., 2004, Linked lowstand delta to basin floor fan deposition, offshore Indonesia: An analogue for deep-water reservoir systems: American Association of Petroleum Geologists Bulletin, v. 88, p. 21–46, doi:10.1306/09030303003.

Savoye, B., and 37 others, 2000, Structure et évolution récente de l'éventail turbiditique du Zaïre: premiers resultants scientifiques des missions d'exploration Zaïango 1 & 2 (marge Congo-Angola). Paris, Academie des Sciences Comptes Rendus, v. 331, p. 211–220.

Schwarz, E., and Arnott, R.W.C., 2007, Anatomy and evolution of a slope channel complex set (Neoproterozoic Isaac Formation, Windermere Supergroup, southern Canadian Cordillera): Implications for reservoir characterization: Journal of Sedimentary Research, v. 77, p. 89–109, doi:10.2110/jsr.2007.015.

Shultz, M.R., Cope, T.D., Fildani, A., and Graham, S.A., 2008, Coarse-grained infill of failure-generated slope accommodation, Tres Pasos Formation, West Face, Sierra Contreras, southern Chile, *in* Nilsen, T., et al., eds., Atlas of deep-water outcrops: American Association of Petroleum Geologists Studies in Geology 56, p, 136–139.

Sixsmith, P.J., Flint, S.S., Wickens, H.D., and Johnson, S.D., 2004, Anatomy and stratigraphic development of a basin floor turbidite system in the Laingsburg Formation, Main Karoo Basin, South Africa: Journal of Sedimentary Research, v. 74, p. 239–254, doi:10.1306/082903740239.

Smith, R., 2004, Silled sub-basins to connected tortuous corridors: Sediment distribution systems on topographically complex sub-aqueous slopes *in* Lomas, S.A., and Joseph, P., eds., Confined turbidite systems: Geological Society of London Special Publication 222, p. 23–43, doi:10.1144/GSL.SP.2004.222.01.03.

Stevenson, C.J., Talling, P.J., Wynn, R.B., Masson, D.G., Hunt, J.E., Frenz, M., Akhmetzhanhov, A., and Cronin, B.T., 2012, The flows that left no trace: Very large-volume turbidity currents that bypassed sediment through submarine channels without eroding the sea floor: Marine and Petroleum Geology, v. 41, p. 186–205.

Straub, K.M., Paola, C., Mohrig, D., Wolinsky, M.A., and George, T., 2009, Compensational stacking of channelized sedimentary deposits: Journal of Sedimentary Research, v. 79, p. 673–688, doi:10.2110/jsr.2009.070.

Sumner, E.J., Talling, P.J., Amy, L.A., Wynn, R.B., Stevenson, C.J., and Frenz, M., 2012, Facies architecture of individual basin-plain turbidites: Comparison with existing models and implications for flow processes: Sedimentology, v. 59, p. 1850–1887, doi:10.1111/j.1365-3091.2012.01329.x.

Tankard, A., Welsink, H., Aukes, P., Newton, R., and Stettler, E., 2009, Tectonic evolution of the Cape and Karoo basins of South Africa: Marine and Petroleum Geology, v. 26, p. 1379–1412, doi:10.1016/j.marpetgeo.2009.01.022.

Twichell, D.C., Schwab, W.C., Nelson, C.H., Lee, H.J., and Kenyon, N.H., 1992, Characteristics of a sandy depositional lobe on the outer Mississippi Fan from SeaMARC IA sidescan sonar images: Geology, v. 20, p. 689–692, doi:10.1130/0091-7613(1992)020<0689:COASDL>2.3.CO;2.

Van der Merwe, W.C., Hodgson, D.M., and Flint, S.S., 2009, Widespread syn-sedimentary deformation on a muddy deep-water basin-floor: The Vischkuil Formation (Permian), Karoo Basin, South Africa: Basin Research, v. 21, p. 389–406, doi:10.1111/j.1365-2117.2009.00396.x.

Van der Merwe, W.C., Flint, S., and Hodgson, D.M., 2010, Sequence stratigraphy of an argillaceous, deepwater basin plain succession: Vischkuil Formation (Permian), Karoo Basin, South Africa: Marine and Petroleum Geology, v. 27, p. 321–333, doi:10.1016/j.marpetgeo.2009.10.007.

Van der Merwe, W.C., Hodgson, D.M., and Flint, S.S., 2011, Origin and terminal architecture of a submarine slide: A case study from the Permian Vischkuil Formation, Karoo Basin, South Africa: Sedimentology, v. 58, p. 2012–2038, doi:10.1111/j.1365-3091.2011.01249.x.

Walker, R.G., 1978, Deep-water sandstone facies and ancient submarine fans: Model for exploration for stratigraphic traps: American Association of Petroleum Geologists Bulletin, v. 62, p. 932–966.

Wynn, R.B., Kenyon, N.H., Stow, D.A.V., Masson, D.G., and Weaver, P.P.E., 2002, Characterization and recognition of deep-water channel-lobe transition zones: American Association of Petroleum Geologists Bulletin, v. 86, p. 1441–1462.